

Positions of hydroxyl masers at 1665 and 1667 MHz

J. L. Caswell[★]

Australia Telescope National Facility, CSIRO, PO Box 76, Epping, NSW 2121, Australia

Accepted 1998 January 17. Received 1998 January 12; in original form 1997 October 27

ABSTRACT

The Australia Telescope Compact Array has been used to observe more than 200 1665-MHz hydroxyl masers south of declination -16° and derive their positions with typical rms uncertainties of 0.4 arcsec. Many of the 1665-MHz maser sites are found to have 1667-MHz OH maser counterparts which are coincident, within the errors.

The resulting position list presented here includes all well-documented, previously reported 1665-MHz masers close to the Galactic plane in the galactic longitude range 230° (through 360°) to 13° . Nearly 50 newly discovered masers are also listed, chiefly in the longitude range 312° to 356° , where the observations were conducted as an intensive survey of a continuous zone close to the Galactic plane.

Many of the maser sites are discussed briefly so as to draw attention to those possessing properties that are unusual among this large sample. Most of the masers are of the variety found in star-forming regions – at the sites of newly formed massive stars and their associated ultracompact H II regions. The new, accurate, positions reveal coincidences of the OH masers with the continuum radio emission, with the infrared emission from dust that accompanies such regions, and with emission from other maser species such as methanol at 6668 MHz and water at 22 GHz.

By-products of the survey, also presented here, include measurements of at least 11 objects that are not associated with massive star-forming regions. They comprise several OH/IR stars (detected at the 1667- or 1665-MHz transition of OH, though commonly found to be most prominent at the 1612-MHz transition) and several unusual masers that may pinpoint other varieties of late-type stars or protoplanetary nebulae.

Key words: masers – stars: formation – H II regions – ISM: molecules – radio lines: ISM.

1 INTRODUCTION

Hydroxyl maser emission at the 1665- and 1667-MHz main-line transitions of the OH ground-state has long been recognized as a valuable tracer of ultracompact H II (ucH II) regions or, more generally, young stellar objects – the sites where massive stars have recently formed. However, many of the previous measurements of southern OH masers had rms position uncertainties greater than 10 arcsec, as measured with a single antenna (e.g. Caswell & Haynes 1987, hereafter CH87), whereas subarcsecond accuracy is needed

to make precise comparisons with other maser species, radio continuum, and IR measurements. Such precision in the southern sky is now attainable (Caswell, Vaile & Forster 1995a, hereafter CVF95) with the Australia Telescope Compact Array (ATCA).

The present ATCA observations consist chiefly of an OH survey that covers the Galactic plane from longitude 312° to 356° ; it yields accurate positions not only for the known 1665-MHz OH masers in this region, but also for the many masers newly discovered in the survey. Outside the survey region, additional observations were made of the known 1665-MHz masers in the wider longitude range 230° through 360° to 13° . Positions measured to an accuracy of

[★]E-mail: jcaswell@atnf.csiro.au

better than 1 arcsec are reported for a prominent feature at each OH maser site, and other associated features are confirmed to usually lie within 1 arcsec of this reference position, apart from a few notable exceptions. Individual masers are discussed, and attention is drawn to those with unusual properties. Preliminary comparisons are made with accurate positions of related objects, and yield some insight into the evolutionary stage of the maser sites.

2 OBSERVATIONS AND DATA REDUCTION

Observations were made with the ATCA in several sessions between 1993 February and 1996 December, in array configurations that yield 15 baselines ranging from 76 to 6000 m. The correlator generated a 2048-channel spectrum across a 4-MHz bandwidth for each of two orthogonal linear polarizations. The main survey was conducted in ‘mosaic mode’ in five 13-h sessions. For each session, a grid of 45 positions over a 9° galactic longitude range, at latitudes 0° and ± 31 arcmin (staggered to give a grid point separation of 36 arcmin) was defined. Each position was observed for typically nine 1.3-min observations spaced over 12 h and interleaved with position calibrators. On other occasions, known 1665-MHz OH masers outside this survey region were observed for typically four periods of 5 min each, again spaced over 12 h.

Processing within the AIPS reduction package involved editing (very little needed), phase calibration, and bandpass calibration. The observations were centred at constant frequency, 1666.0 MHz, but the spectral-line rest frequency of 1665.402 MHz undergoes variable Doppler shifting during the observations owing to the Earth’s motion, and thus the channels had to be realigned using ‘cvel’. The task ‘possm’ was used to inspect scalar-averaged spectra, and the continuum was removed using ‘uvlsf’. Total-intensity maps (the sum of two orthogonal linear polarizations) were produced, first of the channels with maser emission, and then of the continuum, using the average of line-free channels. The synthesized beam has a RA width-to-half-power of ~ 7 arcsec and a declination width of 7 cosec(Dec.) arcsec. The data were Hanning-smoothed to a frequency resolution of 3.9 kHz (0.70 km s^{-1}), and the rms noise on an individual channel map was then typically 40 mJy, allowing detection of sources to ~ 0.16 Jy. However, the survey is not complete to this low limit, since, at this level, a detection is not reliable unless present in several channels, or corroborated by other data. Furthermore, each field was inspected out to, and beyond, the half-power point of the primary beam (radius 15 arcmin), and so the detection level can be several times worse for sources significantly offset from any field centre. The weakest survey source, 316.359 – 0.362, lies close to the expected detection limit, being observed as a peak of 0.15 Jy and corrected for the pointing offset to a peak of 0.2 Jy. For all sources, positions of the strong maser spots in the individual channel maps were measured using ‘imfit’. The continuum maps were inspected for emission from H II regions possibly related to the masers, but the relevant uCH II regions are generally optically thick, and weak, at low frequency; a few detections were made, but require further study at higher frequency before they can be regarded as reliable.

The 4-MHz bandwidth of the observations also allows study of some masers at the other main-line ground-state transition of OH at 1667.359 MHz, although this emission lies within the observed band only if its radial velocity is less negative than approximately -80 km s^{-1} (a limit that depends on source coordinates and observation date).

3 RESULTS

The wealth of detail in the results allows some investigation at each maser site of the distribution of the maser spots with different velocities. However, to explore this thoroughly would require higher spatial and spectral resolution. Furthermore, complete studies would require circular polarization information, since the masers are often highly circularly polarized. (Note that in these ATCA observations we chose to record only two orthogonal polarizations, since circular polarization could not be obtained except at the expense of poorer velocity resolution.) Study of the distributions is thus beyond the scope of this paper, apart from noting that the present data show that the maser spots are confined to groups with typical sizes of less than 1 arcsec. This corroborates previous studies; for example, Forster & Caswell (1989, hereafter FC89) studied 70 maser sites in which they found that the median size of groups of OH maser spots was 0.6 arcsec. Where distances are known, the calculated linear size has rarely been found to exceed 30 mpc ($= 10^{15} \text{ m} = 10^{17} \text{ cm} = 6000 \text{ au}$). Sometimes our maps show a cluster of two or more maser groups, with separations clearly exceeding individual group sizes. It is likely that each compact maser group within such a cluster delineates a separate uCH II region dominated by a massive star, each formed at a similar epoch within a star cluster. In the present work, the position of a prominent reference feature is listed for each maser group. The rms position errors of the observations are estimated to be 0.4 arcsec in each coordinate, an estimate derived principally by comparing measurements at several epochs made for some of the sources, and corroborated by comparisons with VLA positions for 20 masers from FC89 (see also CVF95). Four sources north of declination -20° that were not observed by the ATCA are listed in Table 1 with their FC89 positions. Indirectly confirming the 0.4-arcsec accuracy of the OH positions is the fact that they generally agree with positions of methanol 6668-MHz masers to better than 1 arcsec (Section 5.6).

The OH position measurements are given in Table 1. For each maser group, this lists the peak flux density (of the total intensity) of the reference feature (usually chosen as the strongest feature), its velocity (with respect to the LSR), and its equatorial coordinates (for J2000) as measured in this work. The corresponding galactic coordinates are used as a source name for each maser site. In five cases (330.878 – 0.367, 333.135 – 0.431, 339.682 – 1.207, 339.884 – 1.259 and 358.387 – 0.482), the position of a second spectral feature, separated several arcsec from the first, is listed under the same maser site name (see Section 5.5.4); the size of the group of maser spots at each of these five sites seems to be above average. Four other sites comprise two close pairs where the partners have only slightly different galactic coordinates (330.953 – 0.182 with 330.954 – 0.182 and 331.542 – 0.066 with 331.543 – 0.066) but are thought to be distinct maser sites.

Table 1. Masers at the 1665-MHz OH transition, located south of declination -16° .

OH maser (l, b) (degrees)	RA(2000) (h m s)	Dec(2000) (° ' ")	OH Vpeak (km s ⁻¹)	OH Vrange (km s ⁻¹)	1665MHz Peak (Jy)	1667MHz Peak (Jy)	Epoch of OH	Earlier OH refst	RA(1950) (h m s)	Dec(1950) (° ' ")	Ratio†† m/OH	6668MHz meth refst	6035MHz Peak (Jy)	ucHII flux (mJy)
232.621+0.996	07 32 09.82	-16 58 13.0	21.8	20, 25	1.7(1.7)	0.27	96dec	CBJ88	07 29 54.82	-16 51 45.2	138	C+95; u	<0.1	
240.316+0.071	07 44 51.98	-24 07 42.4	63	62, 68	1.8(1.8)	0.15	95feb	M91	07 42 45.07	-24 00 23.7	<1/8	C+95	2.3	13
263.250+0.514	08 48 47.80	-42 54 28.8	15.3	6, 16	0.42(0.42)	0.5	96oct	T	08 47 00.09	-42 43 18.4	83	S+93; u	<0.15	
*284.177-0.790	10 21 33.87	-58 05 47.6	-27	-36, +16	71(10)	2.1	94nov	AHC80	10 19 45.00	-57 50 37.8				
284.351-0.418	10 24 10.73	-57 52 33.3	5.5	4, 9	0.4	0.8(0.8)	95feb	T	10 22 20.38	-57 37 18.8	<1/5	C97	3.2	<30
285.263-0.050	10 31 29.87	-58 02 18.0	6.5	2, 15	24(24)	[1665/43]	93feb	CH87	10 29 36.67	-57 46 50.9	<1/174	C+95	3.1	<100
287.371+0.644	10 48 04.45	-58 27 01.2	-4	-5, +1	0.6(0.6)	<0.07	95dec	tC96	10 46 04.59	-58 11 09.0	94	C+95; u	<0.15	
290.374+1.661	11 12 18.10	-58 46 20.3	-23.3	-25, -12	1(1)	0.3	96oct	B+89	11 10 07.52	-58 30 00.4	[1.6]	C+95	<0.2	
291.579-0.431	11 15 05.74	-61 09 40.7	13	7, 20	0.84(0.81)	0.75	95feb	CH87	11 12 56.05	-60 53 18.3	[2.8]	C+95	<0.2	
291.610-0.529	11 15 02.59	-61 15 49.5	18	16, 22	6.3(6)	0.8	95feb	CH87	11 12 53.02	-60 59 27.1	<1/22	C+95	<0.25	
294.511-1.621	11 35 32.22	-63 14 42.6	-12.7	-14, -8	30(30)	0.6	94nov	B+89	11 33 13.17	-62 58 06.4	1/2.4	C+95; C97	4.6	< 5
297.660-0.973	12 04 08.99	-63 21 36.0	27	22, 30	1.05(1.05)	0.3	96oct	CH87	12 01 33.59	-63 04 53.5	<1/5	C+95	<0.15	
299.013+0.128	12 17 24.66	-62 29 03.7	20.3	20, 21	1.2(1.2)	<0.1	96oct	CH87	12 14 41.98	-62 12 23.6	[4.9]	C+95	<0.2	
300.504-0.176	12 30 03.49	-62 56 49.8	22.4	3, 24	1.1(1.1)	<0.1	95feb	CH87	12 27 13.52	-62 40 15.1	[2.9]	C+95	<0.2	
300.969+1.147	12 34 53.24	-61 39 40.3	-40	-45, -34	8.0(8.0)	2.4	94nov	CH87	12 32 01.57	-61 23 08.4	1/2.1	C+95; C97	4.6	164
301.136-0.226	12 35 35.07	-63 02 32.4	-38.8	-64, -33	12(12)	4	95feb	CH87	12 32 41.93	-62 46 00.9	[1/11.6]	C+95	<0.15	
305.200+0.019	13 11 16.90	-62 45 54.7	-31.5	-40, -31	1.47(1.0)	<1665/10]	93feb	CH87	13 08 04.49	-62 29 58.1	24	C+95; C97	8.1	<100
305.202+0.208	13 11 10.61	-62 34 37.8	-42.5	-43, -42	0.67(0.67)		93feb	CVF95	13 07 58.56	-62 18 41.1	51	C+95; CVF95	<0.2	
305.208+0.206	13 11 13.78	-62 34 41.1	-38	-44, -36	15.9(15.9)	<1665/20]	93feb	CH87	13 08 01.71	-62 18 44.5	21	C+95; CVF95	<0.2	
305.362+0.150	13 12 35.87	-62 37 17.9	-39.5	-42, -32	10.6(7.6)	[1665/5]	93feb	CH87	13 09 23.00	-62 21 23.0	[1/3.8]	C+95	<0.2	
305.799-0.245	13 16 43.32	-62 58 32.9	-36.7	-37, -34	1.33(1.33)	0.65	96oct	CH87	13 13 27.63	-62 42 43.7	[1/1.7]	C+95	<0.2	
306.322-0.334	13 21 23.00	-63 00 30.4	-22.6	-25, -20	0.4(0.4)	<0.04	96oct	CH87	13 18 04.76	-62 44 47.9	[1/1.9]	C+95	<0.15	
307.805-0.456	13 34 27.40	-62 55 13.8	-16.5	-19, -13	7.5(7.5)	0.2	95feb	CBJ88	13 31 02.45	-62 39 52.2	<1/54	u	<0.2	
308.918+0.123	13 43 01.67	-62 08 51.9	-54	-56, -50	56(56)	11	95feb	CH87	13 39 34.10	-61 53 45.7	1/1.5	C+95; u	<0.15	
309.384-0.135	13 47 24.10	-62 18 12.5	-52	-54, -49	0.23(0.23)	<0.1	96oct	CH87	13 43 54.00	-62 03 14.6	[3.6]	C+95	<0.2	
309.921+0.479	13 50 41.73	-61 35 09.8	-60	-64, -58	27.6(27.6)	1.8	93feb	CH87	13 47 11.72	-61 20 18.4	19.5	C+95; C97	13.4	500
310.144+0.760	13 51 58.26	-61 15 39.5	-52.8	-59, -51	0.25(0.25)	0.15	96dec	T	13 48 28.41	-61 00 50.7	386	vGM95; u		
311.643-0.380	14 06 38.76	-61 58 24.0	38	15, 50	6.8(6.8)	5	95feb	CH87	14 03 00.27	-61 44 06.5	1.5	C+95; C97	0.46	200
311.94+0.14	14 07 48.7	-61 23 22	-41	-42, -40	0.4	<1665]	82feb	CH87	14 04 11.2	-61 09 07	[1]	C+95	<0.2	
312.598+0.045	14 13 15.01	-61 16 53.6	-62	-70, -59	3.6(0.5)	[1665/14]	96jun	CH87	14 09 35.39	-61 02 51.4	[2.7]	C+95	<0.2	
313.469+0.190	14 19 40.98	-60 51 47.1	-10	-11, -6	1.57(0.83)	0.16	96jun	CH87	14 15 59.70	-60 38 00.4	[7.5]	C+95	<0.15	
313.577+0.325	14 20 08.70	-60 41 59.9	-47	-48, -46	0.78(0.22)	<0.4	96jun	T	14 16 27.67	-60 28 14.4	131	vGM95; u		
313.705-0.190	14 22 34.72	-61 08 27.4	-44	-46, -41	0.88(0.53)	<0.2	96jun	T	14 18 51.42	-60 54 48.0	1.5	u		
313.767-0.863	14 25 01.63	-61 44 58.1	-53.5	-57, -49	5.5(5.5)	0.12	95dec	T	14 21 15.48	-61 31 24.8	3.5	S+93; u	<0.15	
314.320+0.112	14 26 26.34	-60 38 31.6	-74	-75, -44	0.61(0.46)	0.25	96jun	T	14 22 42.82	-60 25 02.0	22	S+93; u	<0.15	
316.359-0.362	14 43 11.00	-60 17 15.3	-0.5	-2, 0	0.20(0.15)	<0.1	96jun	T	14 39 21.79	-60 04 30.9	331	C+95; u	<0.2	
316.412-0.308	14 43 23.34	-60 13 00.0	-2	-9, -1	0.32(0.19)	<0.1	96jun	CH87	14 39 34.26	-60 00 16.2	21	C+95; u	<0.15	
316.640-0.087	14 44 18.35	-59 55 11.3	-22	-35, -15	2.64(2.4)	1.1	96jun	CH87	14 40 29.81	-59 42 30.0	33	C+95; u	<0.1	
316.763-0.012	14 44 56.34	-59 48 00.8	-40	-41, -35	1.4(1.4)	0.2	95feb	CH87	14 41 07.92	-59 35 21.4	<1/6	C+95	[0.28]	
316.811-0.057	14 45 26.34	-59 49 15.4	-44	-45, -38	30(28)	0.25	95feb	CH87	14 41 37.67	-59 36 37.4	1/3.6	C+95; u	<0.2	
317.429-0.561	14 51 37.62	-60 00 20.2	25	22, 27	3.87(3.52)	2	96jun	T	14 47 46.06	-59 48 00.2	<1/28	u		
318.044-1.405	14 59 08.74	-60 28 25.7	45	35, 46	0.36(0.36)	0.15	95dec	tC96	14 55 12.90	-60 16 28.1	[14]	C+95	<0.15	
318.050+0.087	14 53 42.69	-59 08 52.6	-53	-55, -48	10.8(5.1)	1	96jun	CH87	14 49 53.00	-58 56 38.8	[1/3.9]	C+95	<0.15	
318.948-0.196	15 00 55.36	-58 58 52.8	-35.5	-42, -30	29.4(19.1)	10	96jun	CH87	14 57 03.67	-58 47 00.9	18	C+95; CVF95	<0.15	<1
319.398-0.012	15 03 17.41	-58 36 12.2	-8.5	-11, -8	[0.75x1667]	0.68(0.45)	96jun	CH87	14 59 26.05	-58 24 27.5	<1/5	C+95	[0.22?]	
319.836-0.196	15 06 54.57	-58 32 57.1	-10.5	-12, -6	0.56(0.19)	<0.3	96jun	CH87	15 03 02.17	-58 21 23.7	[1/2]	C+95	<0.15	
320.120-0.440	15 09 43.85	-58 37 05.8	-55.5	-58, -54	0.7(0.4)	<0.15	96jun	T	15 05 50.32	-58 25 41.3	<1/5	u		
320.232-0.284	15 09 51.96	-58 25 38.3	-67.5	-70, -59	6.5(6.5)	5	95feb	CH87	15 05 58.98	-58 14 14.3	[3]	C+95	<0.15	
321.030-0.485	15 15 51.67	-58 11 18.0	-67	-70, -55	0.52	1.31(1.2)	96jun	T	15 11 57.52	-58 00 13.4	3.1	u	<0.15	
321.148-0.529	15 16 48.39	-58 09 50.2	-63	-65, -60	1.7(1.6)	<0.2	96jun	CH87	15 12 54.03	-57 58 48.7	[3.9]	C+95	<0.15	
322.158+0.636	15 18 34.62	-56 38 25.6	-61	-65, -60	0.68(0.45)	[1665/4]	94nov	CH87	15 14 44.31	-56 27 30.0	214	C+95; CVF95	<0.2	
323.459-0.079	15 29 19.36	-56 31 21.4	-69	-72, -64	8.6(3.6)	2.2	94nov	CH87	15 25 26.38	-56 21 02.0	1.8	C+95; C97	17	449
323.740-0.263	15 31 45.49	-56 30 50.7	-46	-72, -39	1.2	2.5(0.9)	94nov	CBJ88	15 27 51.88	-56 20 39.8	789	C+95; CVF95	<0.15	
324.200+0.121	15 32 52.92	-55 56 07.5	-91.5	-94, -83	13.3(7.2)	12	94nov	CH87	15 29 00.73	-55 46 00.5	<1/96	C+95	<0.2	
324.716+0.342	15 34 57.42	-55 27 24.0	-54	-55, -49	0.43(0.32)	<0.15	94nov	CH87	15 31 06.09	-55 17 24.2	[12.8]	C+95	<0.15	

Table 1 – *continued*

OH maser (l, b) (degrees)	RA(2000) (h m s)	Dec(2000) (° ' ")	OH Vpeak (km s ⁻¹)	OH Vrange (km s ⁻¹)	1665MHz Peak (Jy)	1667MHz Peak (Jy)	Epoch of OH	Earlier OH refs†	RA(1950) (h m s)	Dec(1950) (° ' ")	Ratio†† m/OH	6668MHz meth refs	6035MHz Peak (Jy)	ucHII flux (mJy)
*326.518–0.633	15 49 11.33	-55 08 51.7	-66	-88, -28	4.75(3.8)	3.75	94nov	T	15 45 17.47	-54 59 42.9				
*326.530–0.419	15 48 19.33	-54 58 19.9	-139	-180, -120	1.26(1.15)	?	94nov	T	15 44 26.19	-54 49 07.9				
326.670+0.554	15 44 57.21	-54 07 12.7	-40.8	-41, -40	0.6(0.6)	<0.1	96dec	T	15 41 07.28	-53 57 48.6	<1/2.9	u	<0.15	
326.77–0.26	15 48 56.5	-54 41 50	-58	-59, -57	2.5	<1	78aug	CHG80, T	~15 45 04.1	-54 32 40	<1/8	C+95	<0.2	
*327.102–0.263	15 50 44.76	-54 29 38.8	-90.2	-94, -50	<0.4	3.9(2.05)	94nov	T	15 46 52.46	-54 20 35.7				
327.120+0.511	15 47 32.82	-53 52 39.4	-80.5	-89, -80	6.5(6.5)	0.7	94nov	CHG80	15 43 42.98	-53 43 24.7	9.5	C+95; u	<0.2	<10
327.291–0.578	15 53 07.78	-54 37 06.8	-54.5	-72, -40	15.7(9.6)	1	94nov	CHG80	15 49 14.60	-54 28 12.5	[1/8]	C+95	<0.2	
327.402+0.444	15 49 19.68	-53 45 14.3	-77	-83, -76	2.4(2.4)	[1665/8]	93feb	CHG80	15 45 29.79	-53 36 06.1	[27]	C+95	<0.2	
*328.225+0.042	15 55 20.74	-53 32 44.1	-33	-82, -29	<0.3	1.45(0.8)	94nov	T	15 51 30.15	-53 23 58.1				
328.237–0.547	15 57 58.26	-53 59 22.5	-41	-47, -30	5.7(5.2)	0.44	94nov	CHG80	15 54 05.87	-53 50 46.3	48	C+95; CVF95	[0.58]	
328.254–0.532	15 57 59.80	-53 57 59.6	-37	-54, -35	14.4(13.5)	7.5	94nov	CHG80	15 54 07.47	-53 49 23.4	20	C+95; CVF95	<0.3	
328.307+0.430	15 54 06.48	-53 11 40.3	-92.8	-94, -90	14.4(13.4)	0.4	94nov	CHG80	15 50 17.12	-53 02 49.8	<1/139	C+95	1.4	2600
328.809+0.633	15 55 48.55	-52 43 05.6	-43.5	-50, -35	69.3(52)	10.6	94nov	CHG80	15 52 00.14	-52 34 21.4	3.8	C+95; C97	10.6	360
329.029–0.205	16 00 31.79	-53 12 49.8	-38.5	-42, -36	9.1(4.3)	2.3	94nov	CHG80	15 56 41.08	-53 04 23.2	15	C+95; CVF95	<0.2	
329.029–0.200	16 00 30.38	-53 12 35.5	-38.5	-40, -37	3.3(1.6)	<0.3	94nov	T	15 56 39.69	-53 04 08.8	<1/16	CVF95	<0.2	
329.031–0.198	16 00 30.32	-53 12 27.8	-45.5	-48, -45	1.0(1.0)	<0.2	93feb	T	15 56 39.63	-53 04 01.1	21	C+95; CVF95	<0.2	
329.066–0.308	16 01 09.94	-53 16 02.9	-44	-45, -42	2.45(1.22)	0.7	94nov	T	15 57 18.95	-53 07 38.7	6.7	CVF95; E+96		
329.183–0.314	16 01 47.02	-53 11 43.7	-53	-55, -47	3.8(2.6)	1.5	94nov	CHG80	15 57 56.11	-53 03 21.9	[2.3]	C+95	<0.2	
329.405–0.459	16 03 32.15	-53 09 31.0	-69.5	-76, -67	9.3(7.1)	5.3	94nov	CHG80	15 59 41.01	-53 01 15.8	[11.6]	C+95	[0.15]	
330.878–0.367	16 10 20.01	-52 06 07.7	-61.8	-72, -60	333(190)	61	94mar	CHG80	16 06 30.53	-51 58 18.6	1/800	C+95; u	<0.2	
"	16 10 19.96	-52 06 05.9	-65.6		41.5(23.7)				16 06 30.49	-51 58 16.6				
330.953–0.182	16 09 52.43	-51 54 54.0	-85.5	-95, -80	23.5(15.8)	[0.7x1665]	94mar	CHG80	16 06 03.54	-51 47 03.2	<1/5	C+95; u	[0.38]	
330.954–0.182	16 09 52.78	-51 54 54.2	-97.5	-102, -95	5.2(3.5)	[0.8x1665]	94mar	CHG80	16 06 03.89	-51 47 03.4	<1/37	C+95; u	<0.1	
331.132–0.244	16 10 59.72	-51 50 22.7	-88.5	-94, -88	13.3(10)	[<1665/20]	93feb	CHG80	16 07 10.84	-51 42 36.2	1.5	C+95; u	<0.15	
331.278–0.188	16 11 26.57	-51 41 56.5	-86.8	-92, -78	8.9(8.9)	[1665/3]	94mar	CHG80	16 07 37.99	-51 34 11.7	16	C+95; C96a	<0.25	
331.342–0.346	16 12 26.46	-51 46 16.3	-66.5	-68, -64	5.0(3.9)	2.5	94mar	CHG80	16 08 37.51	-51 38 35.4	[12.7]	C+95	<0.15	
331.442–0.186	16 12 12.41	-51 35 09.5	-83	-84, -82	0.8(0.4)	<0.4	94mar	T	16 08 24.01	-51 27 27.7	70	C96a		
331.512–0.103	16 12 10.12	-51 28 37.7	-91	-94, -85	22.7(22.7)	[0.8x1665]	93feb	CHG80	16 08 22.00	-51 20 55.8	<1/65	C97	1.5	
331.542–0.066	16 12 09.05	-51 25 47.2	-86.5	-87, -83	5.5(5)	[0.7x1665]	94mar	T	16 08 21.07	-51 18 05.3	1/1.1	C+95; C97	4.1	191
331.543–0.066	16 12 09.16	-51 25 45.3	-85.5	-86, -85	2.4(2.2)	<1	94mar	T	16 08 21.17	-51 18 03.3	3.4	C+95; C97	<0.2	<100
331.556–0.121	16 12 27.19	-51 27 38.1	-100	-103, -96	0.96(0.77)	?	94mar	T	16 08 39.07	-51 19 57.3	34	C+95; C97	<0.2	<140
*331.594–0.135	16 12 41.62	-51 26 39.9	-107	-108, -82	4.0(3.6)	?	93feb	T	16 08 53.51	-51 19 00.0		C96a		
332.295+2.280	16 05 41.72	-49 11 30.5	-20	-42, +6	0.86(0.86)	0.7	96dec	IC96; GMv94	16 02 00.43	-49 03 23.9	80	vGM95; u	<10	
332.352–0.117	16 16 07.16	-50 54 30.4	-44	-45, -42	0.77(0.51)	<0.3	94mar	T	16 12 19.90	-50 47 03.9	1/1.1	u		
332.726–0.621	16 20 03.02	-51 00 32.1	-46	-50, -44	0.73	2.4(1.15)	94mar	CHG80	16 16 14.87	-50 53 21.1	[1.5]	C+95	<0.15	
332.824–0.548	16 20 10.23	-50 53 18.1	-54	-55, -53	1.77(0.53)	<0.3	94mar	T	16 16 22.38	-50 46 07.5	<1/17	u		
333.135–0.431	16 21 02.97	-50 35 10.1	-51	-56, -47	40(37)	4.4	94mar	CHG80	16 17 15.78	-50 28 03.1	1/58	C97	7.3	
"	16 21 03.00	-50 35 11.6	-49		7(7)				16 17 15.80	-50 28 04.5			1.1	
333.234–0.060	16 19 50.90	-50 15 10.0	-84	-94, -82	4.2(3)	[<1665/2]	94mar	CHG80	16 16 04.75	-50 07 58.2	<1/20	C96a	<0.2	
333.315+0.105	16 19 29.00	-50 04 41.2	-46	-47, -45	0.66(0.53)	<0.2	94mar	T	16 16 43.36	-49 57 28.0	10	C96a		<43
333.387+0.032	16 20 07.58	-50 04 47.4	-74	-75, -73	0.5(0.5)	<0.15	94mar	T	16 16 21.83	-49 57 36.7	4.7	u		
333.466–0.164	16 21 20.19	-50 09 48.2	-43.5	-48, -36	3.4(3.4)	0.55	94mar	CHG80	16 17 34.04	-50 02 42.3	14	C+95; C96a	<0.15	<40
333.608–0.215	16 22 11.06	-50 05 56.3	-51	-57, -46	11(7.9)	2.8	94mar	CHG80	16 18 24.95	-49 58 53.8	<1/53	C+95	2.1	
335.060–0.427	16 29 23.13	-49 12 26.9	-41	-44, -40	1.4(1.0)	0.35	94mar	T	16 25 38.27	-49 05 53.2	9.9	E+96; u		33
335.556–0.307	16 30 56.00	-48 45 51.0	-113.3	-114, -113	0.08(0.08)	?	96dec	T	16 27 12.04	-48 39 23.6	198	C+95; u	<0.15	
335.585–0.285	16 30 57.33	-48 43 39.9	-48	-49, -39	2.3(2.25)	<0.2	96dec	T	16 27 13.45	-48 37 12.6	7.5	C+95; C96a	<0.2	<40
335.585–0.289	16 30 58.63	-48 43 50.8	-53.5	-60, -49	2.2(2.1)	<0.25	96dec	CHG80	16 27 14.74	-48 37 23.5	10	C+95; C96a	<0.15	<40
335.789+0.174	16 29 47.37	-48 15 51.1	-53	-55, -45	0.45	4.0(2.8)	94mar	CHG80	16 26 04.78	-48 09 19.1	29	C+95; CVF95	<0.2	<40
336.018–0.827	16 35 09.35	-48 46 47.1	-42	-44, -40	0.9	2.6(0.7)	94mar	GMv94	16 31 24.81	-48 40 36.8	109	vGM95; u	<10	
336.358–0.137	16 33 29.16	-48 03 43.7	-82	-84, -80	0.63(0.5)	<0.3	94mar	CHG80	16 29 46.59	-47 57 26.6	23	C+95; C96a	[0.29]	<81
336.822+0.028	16 34 38.26	-47 36 33.0	-75	-79, -74	0.47(0.33)	<0.3	94mar	CHG80	16 30 56.63	-47 30 20.6	23	C+95; C96a	[0.56]	<160
336.864+0.005	16 34 54.39	-47 35 37.2	-88	-90, -86	1.25(1)	?	94mar	T	16 31 12.77	-47 29 25.9	19	C+95; C96a	<0.2	<120
336.941–0.156	16 35 55.22	-47 38 45.7	-68	-70, -65	0.46(0.34)	<0.2	94mar	T	16 32 13.36	-47 32 38.6	51	C96a		<280
336.984–0.183	16 36 12.46	-47 37 55.0	-80.5	-82, -76	0.43(0.3)	<0.4	94mar	T	16 32 30.59	-47 31 49.0	30	C96a		<360
336.994–0.027	16 35 33.95	-47 31 11.4	-121	-125, -114	1.6(1.6)	[<1665]	94mar	CHG80	16 31 52.43	-47 25 02.8	16	C+95; C96a	<0.15	<77
337.258–0.101	16 36 56.36	-47 22 26.8	-70	-72, -68	0.98(0.42)	<0.5	94mar	T	16 33 15.01	-47 16 23.8	10	C96a		<100

Table 1 – *continued*

OH maser (l, b) (degrees)	RA(2000) (h m s)	Dec(2000) (° ' ")	OH Vpeak (km s ⁻¹)	OH Vrange (km s ⁻¹)	1665MHz Peak (Jy)	1667MHz Peak (Jy)	Epoch of OH	Earlier OH refs†	RA(1950) (h m s)	Dec(1950) (° ' ")	Ratio†† m/OH	6668MHz meth refs	6035MHz Peak (Jy)	ucHII flux (mJy)
337.405–0.402	16 38 50.57	-47 27 59.3	-38	-58, -33	66.6(52)	28	94mar	CHG80	16 35 08.79	-47 22 04.1	1	C+95; u	[0.36]	
337.613–0.060	16 38 09.50	-47 04 59.8	-42	-45, -39	1.5(1.4)	<0.15	94mar	CHG80	16 34 28.71	-46 59 01.8	10	C+95; C96a	1.18	<24
337.705–0.053	16 38 29.68	-47 00 35.2	-49	-55, -48	24.7(20.5)	6	94mar	CHG80	16 34 49.02	-46 54 38.6	4	C+95; C96a	0.9	125
*337.860+0.271	16 37 41.49	-46 40 40.5	-81	-85, -48	1.28(0.68)	3	94mar	T	16 34 01.69	-46 34 40.6				
337.916–0.477	16 41 10.43	-47 08 03.1	-52	-54, -31	21(21)	2.6	94mar	CHG80	16 37 29.18	-47 02 17.4	<1/101	C+95	<0.3	
337.920–0.456	16 41 06.07	-47 07 02.4	-39.5	-40, -39	2.06(2.0)	<0.15	94mar	T	16 37 24.86	-47 01 16.4	[16]	C+95	<0.2	
337.997+0.136	16 38 48.48	-46 39 57.6	-35.5	-41, -32	7.7(4.1)	4.7	94mar	CHG80	16 35 08.58	-46 34 02.3	[1/2.8]	C+95	<0.15	
338.075+0.012	16 39 39.05	-46 41 28.0	-47	-53, -44	2.44(2)	0.5	94mar	CHG80	16 35 59.00	-46 35 36.1	5.3	C+95; C96a	[0.43]	1580
338.280+0.542	16 38 09.05	-46 11 03.1	-61	-63, -60	2.3(1.6)	<0.25	94mar	CHG80	16 34 30.33	-46 05 05.1	1.5	C+95; C96a	1.6	<9
338.461–0.245	16 42 15.53	-46 34 18.7	-56	-61, -55	3.3(1.6)	1	94mar	CHG80	16 38 35.48	-46 28 37.5	17	C+95; C96a	<0.15	
338.472+0.289	16 39 58.88	-46 12 35.7	-32	-33, -31	3.8(2.3)	<0.25	94mar	CHG80	16 36 19.90	-46 06 45.3	[1/8]	C+95		
338.681–0.084	16 42 23.99	-46 17 59.4	-22	-23, -19	4.8(3.8)	<0.15	94mar	CHG80	16 38 44.55	-46 12 18.8	<1/46	C+95		
338.875–0.084	16 43 08.23	-46 09 12.8	-36	-41, -33	2.0(1.7)	0.9	94mar	CHG80	16 39 29.05	-46 03 35.3	6.5	C+95; C96a	<0.15	<79
338.925+0.557	16 40 33.57	-45 41 37.2	-61	-65, -57	16.8(11.3)	[1665/50]	94mar	CHG80	16 36 55.69	-45 35 49.1	1/4.8	C+95; u	[0.46]	<15
339.053–0.315	16 44 49.16	-46 10 14.4	-111	-112, -109	0.37(0.25)	?	94mar	T	16 41 09.77	-46 04 43.8	263	C96a		
339.282+0.136	16 43 43.12	-45 42 08.4	-72	-74, -67	0.88(0.63)	<0.25	94mar	T	16 40 04.90	-45 36 33.3	6.9	C96a		<66
339.622–0.121	16 46 06.03	-45 36 43.7	-37.3	-41, -30	20(10)	5	94mar	CHG80	16 42 27.77	-45 31 18.5	2.9	C+95; C96a	[0.69]	<53
339.682–1.207	16 51 06.21	-46 15 57.8	-23	-29, -22	2.3(2.3)	[0.8x1665]	93feb	CH83a	16 47 25.98	-46 10 53.3	1.7	C+95; CVF95; u	<0.15	9
"	16 51 06.20	-46 15 59.8	-25		2.1(2.1)				16 47 25.97	-46 10 55.3				
339.884–1.259	16 52 04.67	-46 08 34.7	-35	-40, -26	9.9(9.9)	[0.7x1665]	93feb	CH83a	16 48 24.64	-46 03 34.3	127	C+95; CVF95; u	<0.15	14
"	16 52 04.64	-46 08 33.5	-29		8.7(8.7)				16 48 24.60	-46 03 33.0				
340.054–0.244	16 48 13.88	-45 21 45.1	-53.6	-59, -47	26(13)	7	95feb	CH83a	16 44 35.98	-45 16 28.7	1.1	C+95; u	<0.15	<80
340.785–0.096	16 50 14.81	-44 42 26.9	-101	-108, -88	6.0(6.0)	[0.4x1665]	95feb	CH83a	16 46 38.18	-44 37 18.9	28	C+95; C97	4.4	9
341.218–0.212	16 52 17.84	-44 26 52.5	-37.3	-42, -35	4.5(2.8)	1.1	95feb	CH83a	16 48 41.59	-44 21 53.1	25	C+95; CVF95	<0.15	140
341.276+0.062	16 51 19.43	-44 13 44.5	-73	-75, -72	0.43(0.33)	<0.15	95feb	CH83a	16 47 43.74	-44 08 41.0	[8.8]	C+95	<0.15	
343.127–0.063	16 58 17.19	-42 52 08.4	-31.5	-41, -29	55(44)	1.3	95feb	CH83a	16 54 43.82	-42 47 34.1	<1/265	C+95	<0.15	
343.930+0.125	17 00 10.92	-42 07 18.7	11.9	10, 14	1.13(0.43)	<0.4	95feb	CH83a	16 56 38.95	-42 02 52.5	10	C+95; C97	3.5	24
344.227–0.569	17 04 07.81	-42 18 40.2	-30.5	-32, -23	1.6(1.6)	1	95feb	CH83a	17 00 35.18	-42 14 30.7	51	C+95; CVF95	<0.15	
344.419+0.044	17 02 08.67	-41 47 08.6	-65	-66, -64	0.5(0.37)	<0.2	95feb	CH83a	16 58 37.25	-41 42 50.8	[22]	C+95	[0.28]	
344.582–0.024	17 02 57.75	-41 41 53.4	-2.3	-11, +2	29(17)	10.5	95feb	CH83a	16 59 26.45	-41 37 39.0	[1/12]	C+95	[0.15]	<60
*344.929+0.014	17 03 56.19	-41 23 59.5	15	-24, +19	< 0.2	8.5(6.9)	95feb	T	17 00 25.43	-41 19 49.3				
345.003–0.224	17 05 11.26	-41 29 06.7	-27	-32, -22	2.7(2.7)	1.4	95feb	CH83a	17 01 40.24	-41 25 01.8	18	C+95; C97	2	233
345.010+1.792	16 56 47.58	-40 14 25.2	-22.5	-31, -15	12.1(12.1)	[1665/3]	93feb	CH83a	16 53 19.58	-40 09 44.9	29	C+95; C97	8.7	260
345.407–0.952	17 09 35.45	-41 35 57.3	-17.6	-19, -17	0.78(0.78)	0.25	96oct	CH83a	17 06 03.93	-41 32 11.0	[2.5]	C+95	[0.26]	
345.437–0.074	17 05 56.59	-41 02 55.6	-24.3	-35, -20	1.65(1.52)	1.8	95feb	T	17 02 26.41	-40 58 53.9	<1/5	u		
345.494+1.469	16 59 41.61	-40 03 43.3	-12.7	-22, -7	3.8(3.8)	0.2	96oct	tc96	16 56 13.75	-39 59 15.2	<1/25	u	<0.15	10
345.498+1.467	16 59 42.81	-40 03 36.2	-15.5	-17, -13	4.6(4.6)	0.45	96oct	tc96	16 56 14.96	-39 59 08.2	1/2.8	u	<0.15	<10
345.504+0.348	17 04 22.87	-40 44 22.9	-19.5	-26, -12	9.8(9.8)	10	95feb	CH83a	17 00 53.39	-40 40 14.6	12	C+95; CVF95	[0.61]	<20
345.698–0.090	17 06 50.62	-40 50 59.4	-6	-9, -2	8.7(8.7)	9.8	95feb	CH83a	17 03 20.77	-40 47 01.5	<1/35	C+95	3.4	<20
346.481+0.132	17 08 22.76	-40 05 25.8	-8	-9, -7	0.85(0.6)	<0.2	95feb	CH83a	17 04 54.30	-40 01 34.5	[2.3]	C+95	<0.15	
347.628+0.148	17 11 51.02	-39 09 29.3	-94.3	-99, -92	9.8(5.5)	[1665/3]	95feb	CH83a	17 08 24.16	-39 05 52.8	1.3	C+95; C97	5.2	160
347.870+0.014	17 13 08.80	-39 02 29.5	-33	-34, -30	2.6(2.4)	<0.15	95feb	CH83a	17 09 42.09	-38 58 58.5	<1/9	u	<0.15	
348.550–0.979	17 19 20.39	-39 03 51.8	-19.7	-22, -10	6.8(4.9)	0.3	96oct	CH83a	17 15 53.34	-39 00 47.4	7.5	C+95; C97	0.9	3
348.579–0.920	17 19 10.56	-39 00 24.5	-27	-28, -26	1.4(1.29)	<0.2	93feb	T	17 15 43.63	-38 57 19.5	1/4.1	u		
348.698–1.027	17 19 58.91	-38 58 14.1	-15.4	-18, -15	0.65(0.65)	<0.1	96oct	CH83a	17 16 32.01	-38 55 12.5	<1/1.9	u	<0.4	
348.703–1.043	17 20 03.96	-38 58 31.3	-16.9	-18, -11	0.22(0.22)	<0.1	96oct	T	17 16 37.05	-38 55 30.1	188	C+95; u	[0.39]	
348.727–1.037	17 20 06.55	-38 57 08.2	-9.2	-12, -2	1.25(1.25)	<0.1	96oct	T	17 16 39.68	-38 54 07.2	50	C+95; u	<0.2	
348.884+0.096	17 15 50.15	-38 10 12.5	-73.2	-76, -71	2.4(1.3)	0.6	95dec	CH83a	17 12 24.94	-38 06 53.2	[2.2]	C+95	<0.2	
348.892–0.180	17 17 00.21	-38 19 27.9	9.5	3, 11	1.29(1.29)	0.4	95dec	CH83a	17 13 34.66	-38 16 13.6	[1.1]	C+95	<0.15	
349.067–0.017	17 16 50.74	-38 05 14.4	15	14, 16	2.0(1.67)	0.25	95dec	CH83a	17 13 25.63	-38 01 59.4	[1/1.5]	C+95	<0.15	
349.092+0.106	17 16 24.59	-37 59 45.5	-80	-91, -79	3.1(2.5)	1.4	95dec	CH83a	17 12 59.67	-37 56 28.7	1.8	C+95; u	<0.15	<70
350.011–1.342	17 25 06.50	-38 04 00.7	-18.3	-27, -17	5.6(5.6)	2.7	96oct	CBJ88	17 21 41.09	-38 01 21.2	[1/8.1]	u(C+95)	<0.15	
350.015+0.433	17 17 45.44	-37 03 12.9	-33	-35, -32	0.81(0.66)	<0.15	95dec	CH83a	17 14 22.18	-37 00 01.9	[5.1]	C+95	<0.2	110
350.113+0.095	17 19 25.58	-37 10 04.5	-71	-77, -65	24.1(20)	1.2	95dec	CH83a	17 16 02.04	-37 07 00.7	<1/70	u	[0.19]	
350.329+0.100	17 20 01.61	-36 59 15.6	-64	-65, -63	0.32(0.25)	<0.15	95dec	T	17 16 38.37	-36 56 14.3	<1.1	u		
350.686–0.491	17 23 28.68	-37 01 48.1	-14.5	-15, -13	0.46(0.32)	<0.15	95dec	T	17 20 05.23	-36 59 01.7	48	vGM95; u	<10	

Table 1 – *continued*

OH maser (l, b) (degrees)	RA(2000) (h m s)	Dec(2000) (° ' ")	OH Vpeak (km s ⁻¹)	OH Vrange (km s ⁻¹)	1665MHz Peak (Jy)	1667MHz Peak (Jy)	Epoch of OH	Earlier OH refs†	RA(1950) (h m s)	Dec(1950) (° ' ")	Ratio†† m/OH	6668MHz meth refs	6035MHz Peak (Jy)	ucHII flux (mJy)
351.160+0.697	17 19 57.35	-35 57 52.4	-8.5	-16, +1	41.6(27)	75	95dec	CH83a	17 16 35.93	-35 54 50.9	[1/10]	C+95	<0.2	<80
351.417+0.645	17 20 53.39	-35 47 01.8	-9.1	-13, -6	108(35)	25	95dec	CH83a	17 17 32.24	-35 44 04.3	21	C+95; C97	140	2800
351.581-0.353	17 25 25.25	-36 12 45.1	-97.6	-101, -89	5.1(3.5)	0.4	95dec	CH83a	17 22 03.18	-36 10 07.1	8.5	C+95; C97	7.8	450
351.775-0.536	17 26 42.56	-36 09 17.6	-2	-29, +8	414(380)	13.5	95dec	CH83a	17 23 20.56	-36 06 45.2	1/2.5	C+95; C97	1.4	3
352.161+0.200	17 24 46.28	-35 25 20.2	-42.2	-43, -41	1.77(0.87)	0.2	95dec	CH83a	17 21 25.62	-35 22 39.5	<1/9	C+95	<0.15	
352.517-0.155	17 27 11.34	-35 19 32.2	-50.6	-56, -43	3.0(2.25)	2.4	95dec	CH83a	17 23 50.77	-35 17 02.0	1.5	C+95; u	<0.2	53
352.630-1.067	17 31 13.91	-35 44 08.4	0	-2, +1	0.22	0.6(0.6)	96oct	T	17 27 52.50	-35 41 55.6	184	S+93; u	<0.2	
353.410-0.360	17 30 26.20	-34 41 45.5	-19.7	-21, -18	12.6(9.7)	<0.15	95dec	CH83a	17 27 06.61	-34 39 29.3	5	C+95; C97	17.5	800
353.464+0.562	17 26 51.56	-34 08 24.8	-45	-46, -43	1.3(1.24)	<0.2	95dec	CH83a	17 23 33.02	-34 05 53.2	6.9	C+95; u	<0.15	<10
354.615+0.472	17 30 17.07	-33 13 54.6	-15.4	-34, -13	4.0(3.65)	2.7	95dec	CH83a	17 26 59.95	-33 11 37.8	37	C+95; CVF95	<0.15	<30
354.724+0.300	17 31 15.52	-33 14 05.3	95	90, 97	0.7(0.7)	0.15	94nov	T	17 27 58.37	-33 11 52.8	20	S+93; C97	0.75	250
*354.884-0.538	17 35 02.70	-33 33 28.7	25	-8, +27	0.6	2.5(1.7)	95dec	T	17 31 44.92	-33 31 32.6				
355.344+0.147	17 33 29.05	-32 47 58.2	19	14, 21	14.3(5.6)	0.4	95dec	CH83a	17 30 12.56	-32 45 55.4	1/2.3	C+95; C97	2.3	570
*356.646-0.321	17 38 40.53	-31 57 18.4	-6.4	-15, +25	2.2(2.1)	1.5	96oct	CH83a	17 35 25.29	-31 55 38.2				
356.662-0.264	17 38 29.22	-31 54 40.6	-54.2	-55, -53	1.57(1.57)	0.6	96oct	CH83a	17 35 14.06	-31 52 59.6	[3.9]	C+95	<0.15	
357.968-0.163	17 41 20.36	-30 45 05.5	-6.3	-10, -4	0.35(0.35)	0.35	96oct	T	17 38 06.99	-30 43 36.9	79	vGM95; u		<10
*358.236+0.115	17 40 54.16	-30 22 37.6	-29	-33, -18	2.6	5.0(0.71)	96oct	CH83a	17 37 41.38	-30 21 05.7				
358.387-0.482	17 43 37.72	-30 33 48.3	-6.3	-7, -5	0.73(0.73)	<0.1	96oct	T	17 40 24.62	-30 32 29.8	2.4	u	<0.15	110
"	17 43 37.95	-30 33 52.0	-7.8	-9, -7	0.4(0.4)	<0.1	96oct	T	17 40 24.84	-30 32 33.4				
359.137+0.032	17 43 25.62	-29 39 17.3	-1	-7, 0	11.2(8.3)	4	95dec	CH83a	17 40 13.93	-29 37 57.9	1.1	C+95; C97	0.73	
359.436-0.103	17 44 40.54	-29 28 15.1	-52	-53, -50	4.05(3.0)	0.35	95dec	CH83a	17 41 29.12	-29 27 01.2	4.6	C+95; C96b	<0.15	<50
359.615-0.243	17 45 39.07	-29 23 29.1	22.5	19, 26	3.07(1.6)	1.5	95dec	CH83a	17 42 27.75	-29 22 19.4	11	C+95; C96b	<0.15	
359.970-0.457	17 47 20.17	-29 11 58.8	15.5	14, 18	10.4(5.9)	<0.4	95dec	CH83a	17 44 09.13	-29 10 56.5	1/15	C+95; C96b	<0.15	<50
0.376+0.040	17 46 21.38	-28 35 39.2	36	28, 40	4.7(4.5)	2.5	95dec	CH83a	17 43 11.27	-28 34 32.7	[1/10]	C+95	<0.15	<70
0.496+0.188	17 46 04.03	-28 24 52.6	-5.5	-7, -5	0.25(0.25)	<0.1	96dec	T	17 42 54.19	-28 23 44.8	36	S+93; C96b		
0.546-0.852	17 50 14.52	-28 54 31.5	13.5	3, 24	3	4.0(4.0)	94nov	CH83a	17 47 03.89	-28 53 41.9	11.7	C+95; u	<0.15	
0.658-0.042	17 47 20.47	-28 23 45.6	67.5	65, 77	137(122)	23	95dec	CH83a	17 44 10.65	-28 22 43.3	<1/397	C96b	<0.3	
0.666-0.035	17 47 20.12	-28 23 06.2	61	48, 62	28.6(25.5)	23	95dec	CH83a	17 44 10.31	-28 22 03.9	<1/83	C96b	2.3	
2.143+0.009	17 50 36.13	-27 05 47.2	59.8	54, 64	6(6)	2	96dec	CH83a	17 47 28.20	-27 04 59.3	[1.15]	C+95	<0.15	<70
3.910+0.001	17 54 38.77	-25 34 45.2	17.5	17, 20	3.6(3.6)	0.2	96dec	CH83b	17 51 33.03	-25 34 15.1	1/2.5	C+95; u	[0.28]	45
5.885-0.392	18 00 30.39	-24 04 04.2	13.9	-44, +19	4.2	15.5(15.5)	96dec	T	17 57 26.77	-24 03 59.7	<1/75	C+95	[0.21]	6
6.048-1.447	18 04 53.15	-24 26 42.2	11.2	10, 12	7.5(7.5)	<0.15	96dec	CBJ88	18 01 48.99	-24 26 56.8	<1/36	C+95	<0.15	
6.795-0.257	18 01 57.72	-23 12 34.6	16.1	13, 18	1.8(1.8)	0.45	96dec	GMV94	17 58 55.29	-23 12 36.5	31	vGM95; u		
8.669-0.356	18 06 19.01	-21 37 32.8	39.2	38, 42	1(1)	<0.2	96dec	T	18 03 18.74	-21 37 53.9	3.9	C+95; u	[0.28]	600
8.683-0.368	18 06 23.46	-21 37 10.2	40	37, 45	2.1(2.1)	1.1	96dec	CH83b	18 03 23.20	-21 37 31.6	49	C+95; u	<0.2	
9.619+0.193	18 06 14.92	-20 31 44.0	5.5	5, 6	3.0(3.0)	<1	96dec	T	18 03 16.12	-20 32 04.8	9.2	u	<0.15	110
9.620+0.194	18 06 14.87	-20 31 36.7	22.5	3, 25	1.4	1.9(1.9)	96dec	CH83b; T	18 03 16.07	-20 31 57.5	<1/5.5	u	<0.2	
9.621+0.196	18 06 14.69	-20 31 32.1	1.4	0, 2	6.8(6.8)	4.1	96dec	CH83b	18 03 15.89	-20 31 52.9	516	C+95; u	<0.15	19
10.444-0.018	18 08 44.88	-19 54 37.9	75.5	74, 77	0.5	2.0(2.0)	94nov	T	18 05 46.90	-19 55 09.7	8.6	C+95; CVF95		
10.473+0.027	18 08 38.25	-19 51 49.4	51.5	48, 69	0.55	1.2(1.2)	94nov	T	18 05 40.33	-19 52 20.7	35	C+95; CVF95	<0.2	142
10.480+0.033	18 08 37.87	-19 51 16.1	66	65, 67	1.0(1.0)	<0.2	94nov	T	18 05 39.97	-19 51 47.3	11	C+95; CVF95	<0.2	
10.623-0.383	18 10 28.61	-19 55 49.1	-2	-3, +1	12.3(1.05)	[1665/2]	94nov	CH83b	18 07 30.61	-19 56 28.4	[1/5]	C+95	[0.22]	3
11.034+0.062	18 09 39.86	-19 21 21.2	21.7	20, 23	6.7	<[1665/10]	83dec	CH83b; FC89	18 06 42.61	-19 21 57.0	[1/13.7]	C+95	[0.24]	
11.904-0.141	18 12 11.56	-18 41 29.6	40.5	40, 43	6.6	[1665/4]	83dec	CH83b; FC89	18 09 15.19	-18 42 16.5	7	C+95; C97	3.2	38
12.03-0.04	18 12 03.6	-18 31 53	109.5	103, 110	3.1	[1665/4]	82feb	CH83b	18 09 07.4	-18 32 39	[26]	C+95	<0.15	
12.216-0.119	18 12 44.45	-18 24 24.6	27.9	21, 31	11	[0.75x1665]	83dec	CH83b; FC89	18 09 48.45	-18 25 13.9	<1/50	C+95; u	<0.15	<150
12.680-0.183	18 13 54.79	-18 01 47.9	64.5	55, 66	10.7(10.7)	6	94nov	CH83b	18 10 59.28	-18 02 42.4	35	C+95; u	<0.15	<60
12.889+0.489	18 11 51.49	-17 31 30.8	33	31, 36	3.6(3.6)	0.35	96dec	CBJ88	18 08 56.62	-17 32 16.3	18	C+95; u	<0.15	
12.908-0.260	18 14 39.53	-17 52 01.1	38	28, 42	63.5(33)	40	94nov	CH83b	18 11 44.23	-17 52 58.8	3.4	C+95; u	<0.15	
15.034-0.677	18 20 24.75	-16 11 34.9	21.5	21, 24	2.5	<[1665/4]	83dec	HCG76; FC89	18 17 31.61	-16 12 57.8	10.8	C+95; C97	14	75

Details of the columns are given in Section 3.

†T refers to a note in text of Section 4. 'u' refers to unpublished data from the ATCA. Other abbreviations are same as defined in reference list.

††m/OH is the ratio of peak methanol (6668 MHz) intensity to peak OH (1665 or 1667 MHz) intensity – see Section 5.6.

*Used to denote the 11 known (or likely) OH/IR or late-type stars, in order to distinguish them from the majority (young star-forming regions).

For those OH maser positions that were measured at several epochs, the listed position is the average. The epoch cited in the table is usually that of the most recent or the 'best' observation for position or flux-density measurement. Also included in the present results are the 47 sources whose preliminary ATCA positions were previously listed by CVF95, in some cases now revised slightly on account of additional data or improved calibration. The accurate J2000 coordinates listed here are recommended for future studies, but the corresponding B1950 coordinates are also listed to allow ready comparison with past work. Some masers discovered a decade ago are now weaker; three (311.94 ± 0.14 , 326.77 ± 0.26 and 12.03 ± 0.04) were not detected in the present observations, but they have been listed in Table 1 for completeness, with the original (relatively low accuracy) Parkes positions. Note that for these positions (with rms errors ~ 10 arcsec), we retain the Parkes Galactic names, with coordinates quoted to centidegrees rather than millidegrees.

Many of the maser sites are significantly offset from the pointing direction of the primary beam, and the flux density listed has been increased to correct for this offset (with the measured, uncorrected flux density shown in parentheses). The positional accuracy is not adversely affected by large offsets unless the measured source amplitude is greatly reduced and results in a very low value of the signal-to-noise ratio.

Spectra from the present ATCA observations are shown in Fig. 1 for a few sources, selected to display their considerable variety. Masers of the star-forming-region (SFR) type dominate our survey, and several examples are shown, e.g., 345.494 ± 1.469 and 345.498 ± 1.467 , a pair separated by only 18 arcsec and probably in the same cluster. The SFR masers usually have a quite small velocity range (314.320 ± 0.112 is an exception) and are usually considerably stronger at 1665 than at 1667 MHz (332.295 ± 2.280 is an exception). 326.518 ± 0.633 is apparently an unusual late-type star, strongest at the 1612-MHz transition and with velocity structure indicative of a double expanding shell. 326.530 ± 0.419 and 356.646 ± 0.321 are also probably unusual late-type stars. The classification of 345.437 ± 0.074 is unclear.

The present ATCA spectra have quite high sensitivity, but, for masers in SFRs especially, spectra with higher velocity resolution and showing separately the right- and left-hand circular polarizations (RHCP and LHCP) are often more informative. Such a set of current spectra is not available, but detailed spectra from earlier epochs for many of the OH masers can be seen in CH87, Caswell, Haynes & Goss (1980, hereafter CHG80) and Caswell & Haynes (1983a,b, hereafter CH83a, CH83b) for longitude ranges 305° – 326° , 326° – 339° , 339° – 2° and 3° – 13° , respectively. In Table 1, references are given to such published spectra of known sources, and sometimes refer to the present text (notes of Section 4), especially for more complex spectra which are not adequately characterized by the peak and velocity range of the emission. The velocity range of emission cited in Table 1 is the total range over which 1665- or 1667-MHz maser emission has been detected.

The OH peak flux densities listed in Table 1 from the present data are total intensity values at relatively low spectral resolution, and are usually lower than those seen on

high-resolution spectra. The ratio of the flux density in Table 1 relative to the peak value from a high-resolution spectrum was calculated for 160 sources where this was possible. Apart from the random effect of variability when spectra are at different epochs, this ratio is the net effect, on the one hand, of poorer resolution and, on the other hand, of the effects of polarization, since the peaks of Table 1 are total intensity, whereas those from high-resolution spectra are for the stronger sense of circular polarization. The ratio lies between 0.4 and 1.0 for 60 per cent of the sources, with a median value of 0.69. In the absence of a more detailed spectrum, the peak intensity from Table 1 should be increased by typically $1/0.69 = 1.45$ if it is to be incorporated with statistics that have been derived mainly from high-resolution spectra (see Section 5.6).

The survey was intended primarily for the study of 1665-MHz masers, but the 1667-MHz transition can often be observed near the edge of the band. When detected, the 1667-MHz peak intensity is listed in Table 1. It is usually weaker than the 1665-MHz transition for masers of the type studied here (see Section 5.4), but is sometimes stronger and can then provide especially useful additional information. Where the 1667-MHz emission is significantly stronger than 1665-MHz emission, it is used to derive the position for Table 1, and its velocity is given as the velocity of the peak. Such cases are discussed in the notes in Section 4.

Some of the ground-state OH measurements of Table 1 are not from the present observations. Examples include the 1667-MHz flux density for some sources; it is then cited as a fraction of the 1665-MHz intensity (and enclosed in square brackets), since the actual value measured with frequency resolution not matching that at 1665-MHz would be misleading. Table 1 also lists information on associated masers at the 6035-MHz OH transition as detailed in Section 5.4, methanol 6668-MHz masers as detailed in Section 5.6, and uCH II regions as detailed in Section 5.7.

4 INDIVIDUAL SOURCES

With the exception of one very weak source, the peak flux densities of 1665-MHz masers in Table 1 range from 0.2 to 500 Jy, with a median value of 2.7 Jy. The weakest OH maser tabulated is the 0.08-Jy newly reported source 335.556 ± 0.307 , measured with long integration at the ATCA, following its discovery from sensitive single-dish observations made with the Parkes telescope. The strongest is 351.775 ± 0.536 , for which our measured peak was ~ 500 Jy in 1995 December, and which at higher frequency resolution exceeds 1000 Jy, the strongest 1665-MHz OH maser known.

Additional information on some of the sources is presented in the remainder of this section. In particular, attention is drawn to several small clusters, and to individual masers with accompanying emission at the 1612- or 1720-MHz OH ground-state transitions and the 6035-MHz transition of excited OH. Intensity variations often occur over several years, and where they have been unusually large, we draw attention to this, especially if new features extend the previously estimated velocity range of the emission. Most of the masers occur in SFRs (see Section 5.1) and have methanol maser counterparts (e.g. Caswell et al.

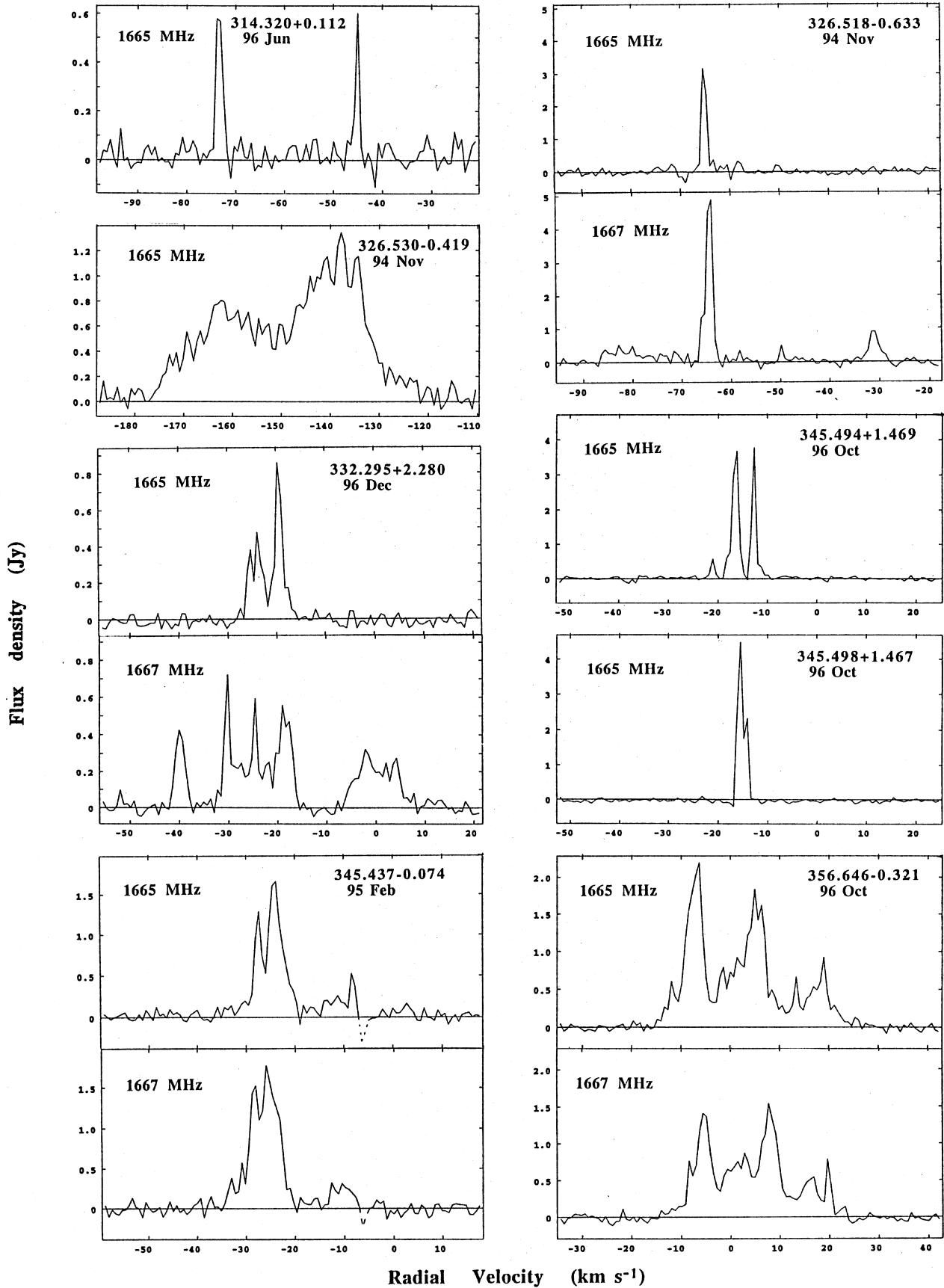


Figure 1. Spectra of selected OH masers (see Section 3, and Section 4 for notes on each source). Each spectrum shows the total intensity (Stokes I) and spans a velocity range of 75 km s⁻¹ with a resolution 0.7 km s⁻¹.

1995c, hereafter C + 95) as discussed in Section 5.6; we draw attention to several exceptions. We also discuss individually the 11 masers (marked with an asterisk) that are members of the OH/IR late-type star or protoplanetary-nebula variety (see also Section 5.1).

The discussion of individual sources is an integral part of this study, but some readers may now wish to jump to the ensuing generalizations of Section 5, and return to consult the remainder of this section when references are made to individual sources.

232.621 + 0.996. 1665-MHz emission from this site was first reported by Cohen, Baart & Jonas (1988, hereafter CBJ88, but with position error as noted in their subsequent erratum), emitting from two features primarily LHCP. Our Parkes (unpublished) spectra show that the initially weaker feature at velocity 21.8 km s^{-1} increased slightly from 1989 through 1992 to 1996 and is now the strongest, while the previously strongest feature (2.5 Jy in 1992 at 23.5 km s^{-1}) has now weakened. Weak 1667-MHz emission is discernible for the first time on the ATCS spectrum. The methanol maser counterpart reported by C + 95 is now confirmed as coincident with the OH, from unpublished ATCA methanol observations (the unpublished ATCA data referred to here and later are recent observations by the author).

263.250 + 0.514. This new source was first detected at Parkes as two features, both LHCP, at 1665 MHz; the ATCA observation shows emission of comparable intensity at 1667 MHz also. A methanol maser reported by Schutte et al. (1993, hereafter S + 93) is confirmed from ATCA data to be coincident.

**284.177 – 0.790.* This is an unusual maser located in the bipolar nebula Roberts 22 (Allen, Hyland & Caswell 1980, hereafter AHC80). The present observations have the highest positional precision yet achieved and reveal that OH emission is distributed over several arcsec, within a region encompassed by the nebula. The OH maser emission is strong at both 1665 and 1612 MHz. The evolutionary status of this source is still a matter of dispute, but it is commonly categorized with the OH/IR late-type stars and protoplanetary nebulae.

284.351 – 0.418. The present observations yield a precise position and show this maser to be stronger at 1667 MHz than at 1665 MHz (it was first reported by CH87 as a marginal, probable non-detection!). There is an excited-state 6035-MHz OH counterpart (Caswell 1997, hereafter C97) which is variable and currently stronger than any other transition, but the site has no methanol emission, although there is a methanol maser at a separate site displaced 5 arcsec.

291.579 – 0.431. As noted by CH87, the 1665-MHz maser has been as strong as 8.5 Jy . Currently it is below 1 Jy (but strong enough to measure a precise position), and there is slightly weaker emission at velocity $+7 \text{ km s}^{-1}$ detected from the 1667-MHz transition.

300.504 – 0.176. The peak emission at 1665 MHz is at velocity 22.4 km s^{-1} . There is also a weak feature at 4 km s^{-1} (outside the range of the spectrum shown by CH87), and thus the velocity range of the emission is much wider than the typical value of 9 km s^{-1} (see Section 5.5.3).

301.136 – 0.226. Spectra from CH87 show emission over the large velocity range from -35 to -64 km s^{-1} . The weak outlying features are not detectable on the ATCA

1665-MHz spectrum, but a weak feature near -50 km s^{-1} is quite prominent and is confirmed to be very close to the main emission, with an offset of only 1 arcsec.

305.202 + 0.208 and 305.208 + 0.206. The second source is a strong maser shown in CH87; the first is a weak companion first noted by CVF95. Both OH masers have methanol counterparts (CVF95).

306.322 – 0.334. This maser was first detected with a peak of 2 Jy by CH87 in 1980, but it faded and became barely detectable by 1982. Subsequent Parkes spectra show emission of nearly 1 Jy in 1990 and 1992, and the present ATCA observation provides the first precise position. A 1720-MHz maser has also recently been detected from approximately this direction (MacLeod 1997).

307.805 – 0.456. When the discovery of this maser was reported by Cohen et al. (1988), the position error was greater than 15 arcmin. The present improved OH position was used to search for methanol, and yielded the upper limit shown in Table 1.

310.144 + 0.760. This is a weak new OH maser, and a methanol maser reported by van der Walt, Gaylard & MacLeod (1995, hereafter vGM95) is found to coincide with it (using a newly determined precise methanol position from the ATCA).

311.643 – 0.380. This was first reported by CH87, showing emission at both 1665 and 1667 MHz with comparable intensity. The large positive systemic velocity shows that it is outside the solar circle, at a very large distance of 16.3 kpc. The velocity spread is found from the present data to be remarkably wide, from $+15$ to $+50 \text{ km s}^{-1}$. The strongest features from $+30$ to $+40 \text{ km s}^{-1}$ were seen in the CH87 Parkes spectrum, but the weaker ‘plateau’ of $\sim 0.2 \text{ Jy}$ seen in the present ATCA data was not evident because the limited extent of the earlier spectrum made it difficult to define the baseline. Features at the extreme velocities lie within 1 arcsec of the main central emission. Associated masers of OH at 6035 MHz and methanol at 6668 MHz have recently been mapped (C97), and are coincident with the present 1665-MHz position; an additional 6035-MHz maser is present at a position 182 arcsec away (at $311.596 – 0.398$) where no other masers are detectable (see Section 5.4).

311.94 + 0.14 (311.944 + 0.136). This source was reported by CH87, but was not detectable ($< 0.14 \text{ Jy}$) in the current ATCA observations. Parkes observations on several occasions have shown the source to be 0.4 to 0.6 Jy in LHCP at velocity -41 km s^{-1} , and it is therefore listed in Table 1 (with the low-accuracy Parkes position) for completeness. The weak (0.6 Jy) methanol counterpart reported by C + 95 is nominally offset by 1 arcmin to larger RA and north, but is quite likely coincident in view of the uncertainties.

313.577 + 0.325. This is a new weak OH maser coinciding with a strong methanol maser (vGM95 and unpublished ATCA data).

313.705 – 0.190. This new OH maser is found to have a weak methanol counterpart (unpublished ATCA data).

313.767 – 0.863. Unpublished Parkes observations show that 1665-MHz emission is present not only in LHCP (as first reported by Gaylard & Whitelock 1988, and also Gaylard, MacLeod & van der Walt 1994, hereafter GMv94) but also, slightly weaker, in RHCP. A nearby methanol maser reported by S + 93 is found (from unpublished ATCA

observations) to have one component coincident with the OH maser position reported here, and another at a position offset 25 arcsec.

314.320 + 0.112. This new OH maser is remarkable in possessing two prominent features which have a large separation in velocity of nearly 30 km s^{-1} (see Fig. 1), and yet which are found to be at the same position. A methanol maser reported by S + 93 is found (from unpublished ATCA measurements) to coincide with the OH, and extends over the substantial velocity range -43 to -60 km s^{-1} .

316.359 - 0.362. This is one of the weakest new OH masers, and its detection in preliminary Parkes observations was mentioned by C + 95. An improved position for the strong methanol counterpart reported by C + 95 shows it to coincide with the OH to within 2 arcsec (satisfactory agreement in view of the faintness of the OH signal).

316.412 - 0.308. The weak 1665-MHz emission from this source has features at -7.5 km s^{-1} (position given by CVF95 from observations 1993 February) and at -2 km s^{-1} as measured in the present observations (1996 June), which are essentially coincident.

316.640 - 0.087. A preliminary ATCA position was given by CVF95. Additional new data confirm the position, and show that the velocity range of the emission is very wide. It extends from velocity -15 to -35 km s^{-1} at both 1667 and 1665 MHz. The weak extension from -28 to -35 km s^{-1} was not evident in the Parkes spectra shown by CH87 because of the greater difficulty in establishing a precise baseline for single-dish observations. The methanol maser reported by C + 95 is confirmed (unpublished ATCA data) to be coincident with the OH.

316.811 - 0.057. A spectrum recorded in 1982 February is shown by CH87; the feature at velocity -43.5 km s^{-1} , which was then less than 4 Jy, has shown enormous variability, reaching 20 Jy in 1989 November (Parkes unpublished data) and 30 Jy in 1995 February and 1996 June (present data).

317.429 - 0.561. This new maser is of special interest, because its large positive velocity of 25 km s^{-1} suggests that it is at an unambiguously large distance, outside the solar circle. There is no associated methanol maser (less than 0.2 Jy in unpublished ATCA observations), and so there is an alternative, but less likely, possibility that the OH maser emission is from a late-type star, for which anomalous velocities are not uncommon.

318.044 - 1.405. This weak maser was discovered by te Lintel Hekkert & Chapman (1996, hereafter tC96) when searching at the position of IRAS 14551 - 6016, but our accurate maser position suggests that it is not a precise counterpart to the IRAS source. The large positive velocity of this OH maser, like the previous one, is indicative of a large and unambiguous distance. There is a weak methanol counterpart.

318.948 - 0.196. This OH maser is highly variable, falling to less than 2 Jy in 1982 February, flaring to more than 40 Jy in 1989, and again high, at both 1665 and 1667 MHz, in the present 1996 June observations. Methanol is very strong (780 Jy) and coincides with the OH (CVF95), but there is no detectable ucH II region here (Ellingsen, Norris & McCulloch 1996a report a limit below 1 mJy for the peak of any emission at 8.5 GHz).

319.398 - 0.012. OH maser emission here is stronger at 1667 MHz than at 1665 MHz, and measurements at the OH 6035-MHz transition show a possible marginal detection of 0.22 Jy RHCP at velocity -12.7 km s^{-1} . Methanol is not detectable here.

319.836 - 0.196. Variable OH emission showed a peak at 1665 MHz of 1.5 Jy in 1982, flaring in 1989 September to 5 Jy (pure LHCP) but below 1 Jy in 1996; at 1667 MHz it is currently below the detection threshold. Weak methanol (0.4 Jy reported by C + 95) appears to coincide with the OH.

320.120 - 0.440. This is a new weak maser with no detectable methanol (unpublished ATCA data show $< 0.2 \text{ Jy}$).

320.232 - 0.284. Most of the OH emission here has been stable, but a 1665-MHz RHCP peak at velocity -67.5 km s^{-1} varied from 20 Jy (1982) to 30 Jy (1989) to $\sim 10 \text{ Jy}$ (1996).

321.030 - 0.485. This new OH maser is strongest at the 1667-MHz transition. It has a weak methanol counterpart of 6 Jy, discovered in new ATCA observations. The new ATCA observations also reveal that a strong methanol maser reported by S + 93 is offset 15 arcsec from 321.030 - 0.485, and thus is clearly a different maser site, but it has a similar velocity range, and most likely resides in the same star-forming cluster.

321.148 - 0.529. Spectra at 1665 and 1667 MHz obtained with the Parkes telescope are shown by CH87. The weak 1667-MHz feature that they reported is not seen in the present data and, in hindsight, was probably a sidelobe response to emission from 321.030 - 0.485.

323.459 - 0.079. Note that there is also emission from the OH 1612-MHz transition here; the accurate 1612-MHz position (Sevenster et al. 1997b, hereafter S + 97) coincides with the 1665-, 1667- and 6035-MHz OH emission, and with 6668-MHz emission from methanol (C97). It is uncommon to find the 1612-MHz OH and methanol coincident, as discussed in Section 5.4.

323.740 - 0.263. This OH maser, first reported by CBJ88, is stronger at 1667 MHz than at 1665 MHz. It is especially interesting for its variability and wide velocity spread, showing many features from -39 to at least -62 km s^{-1} . This range is extended still further by a new 1665-MHz feature at -72 km s^{-1} , which is currently the strongest emission, being a flare between 1993 February (when it was $< 50 \text{ mJy}$) and 1994 November (when it rose to 1.2 Jy to become the strongest feature of the 1665-MHz spectrum). At this site there is a methanol maser counterpart, which is one of the strongest known.

**326.518 - 0.633.* This appears to be an OH/IR star that is unusual in having two expanding shells (see Fig. 1 for 1665- and 1667-MHz spectra), and it has also been detected by S + 97 at 1612 MHz, where its peak intensity is twice the 1667-MHz value.

**326.530 - 0.419.* The spectrum of this maser at 1665 MHz (shown in Fig. 1) has unusually wide emission centred at large negative velocity and lying in the velocity range not covered at 1667 MHz. Like the previous source, a 1612-MHz counterpart with velocity structure matching that at 1665 MHz (although weaker than at 1665 MHz) has been reported by S + 97. It is probably a late-type star, but there is no positional agreement with any IRAS source.

326.670 + 0.544. This is a weak new OH maser site at which no methanol (<0.3 Jy) was present in an unpublished ATCA search; the ATCA observations showed that a strong methanol maser, 326.63 + 0.60 (reported by S + 93) and by Ellingsen et al. 1996b, hereafter E + 96) is offset by several arcmin from the OH site.

326.77 – 0.26. This source, reported by CHG80 as showing intensity variations by a factor of 3 over 2 yr, was not detectable in the current ATCA observations, and is listed in Table 1 with the original Parkes low-accuracy position.

*327.102 – 0.263. Detected at 1667 MHz but not at 1665 MHz, this maser corresponds to an OH/IR star strongest at 1612 MHz, and first reported by Caswell & Haynes (1975, hereafter CH75), with an improved position derived by S + 97. The 1667-MHz emission is primarily near velocity -90 km s^{-1} (which, at 1612 MHz, is the lesser of the two peaks) and only marginally present near velocity -54 km s^{-1} (the stronger 1612-MHz peak).

327.291 – 0.578. Spectra shown by CHG80 reveal emission over a wide velocity range and with marked intensity variations, which subsequent Parkes monitoring has shown to be common in this source. The accurate OH position reported here agrees with a new (ATCA unpublished) position for the weak associated methanol maser.

*328.225 + 0.042. This is relatively weak 1667-MHz emission from an OH/IR star that emits 40 times more strongly at 1612 MHz (CH75; S + 97).

328.237 – 0.547 and 328.254 – 0.532. The Parkes spectra of CHG80 show a blend of these two masers which are separated by 84 arcsec. The present ATCA data show the first source to have a wide velocity range of -47 to -30 km s^{-1} , matching its methanol counterpart (C + 95; CVF95). The second OH maser has a main feature that has varied by a factor of 2, and shows a slightly wider velocity range, -54 to -35 km s^{-1} , also matching its methanol counterpart (C + 95; CVF95).

329.029 – 0.205, 329.029 – 0.200 and 329.031 – 0.198. Referred to by CVF95 as 329.03 – 0.21, 329.03 – 0.20 and 329.03 – 0.20s respectively, these three sites are so close that they are all present, but blended together, in the CHG80 spectrum of 329.04 – 0.21. The first and third OH masers have methanol counterparts (C + 95; CVF95).

329.066 – 0.308. This site was discovered by CVF95 as both an OH maser and a methanol maser (referred to as 329.07 – 0.31). The OH emission is primarily from a single feature, whereas methanol features at several velocities are present, as seen in the recent spectrum from E + 96.

330.878 – 0.367. OH spectra at 1665 and 1667 MHz (CHG80) show many strong features in the velocity range -72 to -60 km s^{-1} . The present ATCA measurements show that the features are distributed over several arcsec, and two positions are listed in Table 1 to demonstrate the extent of the spread. None the less, the emission seems best described as a single, quite extended, maser site rather than two separate ones, although verification will require maps of higher spatial resolution covering both circular polarizations with high velocity resolution. The weak 1612-MHz OH emission at this site, with velocity -62.9 km s^{-1} , was once thought to be quasi-thermal, but new, high-resolution, precise measurements (S + 97) show it to be a weak maser. S + 97 also reported an additional very weak 1612-MHz feature, which is either quite remarkable in view of its enor-

mous offset in velocity to -163.6 km s^{-1} , or else, more likely, is unrelated. Methanol emission of 0.8 Jy is reported by C + 95; ATCA methanol measurements show a weak 0.6-Jy feature within 1.8 arcsec of the OH position, and reveal that a slightly stronger methanol feature seen on the C + 95 spectrum is from a separate site, offset more than 60 arcsec.

330.953 – 0.182 and 330.954 – 0.182. The spectrum (labelled 330.96 – 0.18) from CHG80 shows both masers. The ATCA positions distinguished the first source as corresponding to the features in the velocity range -95 to -80 km s^{-1} ; the second source, offset 3.3 arcsec, constitutes features with velocity more negative than -95 km s^{-1} . Neither OH site has associated methanol, and the methanol reported by C + 95 comes from yet a third site, offset 3 arcsec, according to new ATCA measurements. Thus there are at least three maser sites in this cluster, and it is likely that strong extended H II at this position (integrated flux density 1.64 Jy) may be only loosely related to the masers, and could obscure any weaker compact H II more directly associated.

331.278 – 0.188. A spectrum taken 1978 August is shown by CHG80; the most recent spectra are generally similar, with peak intensity 8.9 Jy, although a remarkable flare to at least 26 Jy occurred during 1990 January.

331.442 – 0.186. This is a new OH maser, with an accompanying strong methanol maser (vGM95; Caswell 1996a, hereafter C96a).

331.512 – 0.103. Most of the features seen on the CHG80 Parkes spectra at 1665 and 1667 MHz of 331.52 – 0.10 arise from this position. At 6035 MHz there is a maser coincident with the 1665-MHz position and an additional, stronger, one with more spectral features (331.511 – 0.102, offset 1.7 arcsec from 331.512 – 0.103), which may be a separate maser site without 1665-MHz emission (C97). Unusually strong 1612-MHz maser emission here has been known for several decades, and its recently determined position (S + 97) shows that it coincides with the main 1665-MHz source. There is no methanol maser in the vicinity (C97), an example of the tendency for 1612-MHz OH masers and 6668-MHz methanol masers to be mutually exclusive (see Sections 5.4 and 5.6).

331.542 – 0.066 and 331.543 – 0.066. This is a close pair of maser sites separated by 3 arcsec. Complementary observations at higher frequency (C96a; C97) show that 331.542 – 0.066, the stronger maser at 1665 MHz, is associated with a uCH II region of 191 mJy and has accompanying masers at the 6035-MHz OH and 6668-MHz methanol transitions; the close neighbour to the north, 331.543 – 0.066, has a methanol counterpart but no detectable H II region or 6035-MHz emission.

331.556 – 0.121. This new maser may have been responsible for the weak emission seen near velocity -100 km s^{-1} on the 1978 spectrum of 331.52 – 0.10 at 1665 MHz (CHG80). A methanol maser coincides.

*331.594 – 0.135. This is a new 1665-MHz maser with wide velocity range, although its strongest emission is confined to a much smaller range. A 1612-MHz OH maser coincides in position and has a velocity structure characteristic of an OH/IR late-type star (S + 97, although there is confusion in their spectrum from a nearby strong source). There is no methanol detected here (< 1 Jy from the survey

data of C96a), and indeed, no methanol has yet been detected towards any OH/IR late-type star.

332.295 + 2.280. This maser has a quite remarkably wide spectrum, as shown in Fig. 1. Its detection was reported by GMv94 (but the wide velocity was not clear) and by tC96 but with no precise position, whereas we now confirm that the 1665- and 1667-MHz features all arise from a single compact site. 1612-MHz emission is shown by tC96, but the fact that it is absent from the S + 97 survey suggests that it may be extended and not associated with the 1665- and 1667-MHz maser site at 332.295 + 2.280. However, we find (unpublished ATCA observations) that the strong methanol maser reported by vGM95 does coincide with 332.295 + 2.280.

332.352 – 0.117. This new OH maser has a weak, 1-Jy, methanol counterpart which was not reported by C96a, since it was detected with only marginal significance and has only recently been confirmed.

332.726 – 0.621. In this maser the emission at 1667 MHz is 3 times stronger than at 1665 MHz (see also the spectra shown in CHG80).

332.824 – 0.548. This is a new 1665-MHz maser which has no methanol counterpart (< 0.2 Jy), although there is a 1.6-Jy methanol maser offset by 7 arcsec (unpublished ATCA data).

333.135 – 0.431. This is a well-known strong maser (CHG80), and positions for two features have been listed. Provisionally, we treat it as a single extended site, although it might be two distinct but nearby sites. There are also two positions of emission at 6035-MHz (as discussed by C97), and weak emission from a methanol maser.

333.234 – 0.060. The OH 1665-MHz position measured here agrees closely with the position of an associated 1612-MHz maser (S + 97). There is no methanol maser at this site, the nearest one being 333.234 – 0.062, which is clearly offset by 7 arcsec (C96a).

333.315 + 0.105. This is a newly detected OH maser, which has a coincident methanol maser (C96a).

333.387 + 0.032. This new OH maser has a new methanol maser counterpart detected in recent unpublished ATCA observations.

333.608 – 0.215. This is a maser site towards an H II region that is very prominent in the IR and radio continuum (C97). Spectra of OH at 1665 and 1667 MHz are displayed by CHG80. The present position shows that 1665- and 1667-MHz emission coincides with 6035-MHz OH (C97) and with a 1612-MHz maser (S + 97). There is no associated methanol maser (< 0.3 Jy according to C + 95).

335.060 – 0.427. The position of only the main feature of this new maser is given in Table 1, but a second feature, though blended with it and weak, is clearly offset north by at least 2 arcsec. There is a methanol maser at the position of the main OH feature, with spectrum shown by E + 96 and position from unpublished ATCA data.

335.556 – 0.307. This new OH maser is the weakest in our list, and its velocity of -113.3 km s $^{-1}$ implies a large unambiguous distance near the tangent point. It was detected after a deep search at the site of a methanol maser discovered by C + 95 (with accurate position determined from unpublished ATCA observations).

335.585 – 0.285 and 335.585 – 0.289. The two masers are separated by 15 arcsec. The first one is stronger, and an

early spectrum is seen in CHG80, where the source was labelled 335.61 – 0.31. There is a methanol maser at both sites and a third methanol maser very nearby, within the same cluster (C96a).

335.789 + 0.174. Current spectra remain similar to those shown by CHG80, with 1667-MHz emission strongest, and 1665-MHz emission covering a slightly wider velocity range, from -55 to -45 km s $^{-1}$. CVF95 confirm that the methanol counterpart shown by C + 95 coincides with the OH position.

336.018 – 0.827. This was first reported by GMv94, and shows 1667-MHz features stronger than 1665-MHz features. The present OH position coincides with a new ATCA unpublished position for the strong methanol counterpart (vGM95).

336.822 + 0.028 and 336.864 + 0.005. The first of these, referred to as 336.83 + 0.02 and with peak at velocity -78.6 km s $^{-1}$ when observed in 1978 by CHG80 is now weaker, with its peak at a velocity of -75 km s $^{-1}$. The second is a new OH maser, probably corresponding to weak features near velocity -88 km s $^{-1}$ which were offset from the beam centre in the CHG80 spectrum of 336.83 + 0.02. Both OH masers have methanol counterparts (C + 95; C96a).

336.941 – 0.156. This is a new OH maser, with methanol counterpart (C96a).

336.984 – 0.183. This new maser appears to be 3.2 arcsec south of a possible methanol counterpart (C96a), and it is not clear whether this offset might simply indicate that the position error for the OH maser is larger than usual because it is weak.

337.258 – 0.101. This is a new OH maser, with methanol counterpart (C96a).

337.405 – 0.402. Spectra at both 1665 and 1667 MHz show features over a wide velocity range (CHG80), and over 20 yr have remained at similar velocities but have shown intensity variations. Both the 1665- and 1667-MHz masers occur in two velocity ranges (at -55 and -35 km s $^{-1}$), all now measured to be at nearly the same position. The methanol counterpart (C + 95) has features confined to the velocity range from -43 to -36 km s $^{-1}$.

***337.860 + 0.271.** The 1667- and 1665-MHz maser emission reported here is the counterpart of an OH/IR star, which we find to be almost as strong at 1667 MHz as at 1612 MHz (CH75; S + 97).

337.916 – 0.477 and 337.920 – 0.456. These sources are separated by 75 arcsec. The first is the stronger and accounts for most of the emission seen on the spectrum at 337.92 – 0.46 shown by CHG80. The velocity range is wide, extending from -54 to -31 km s $^{-1}$. There is no detected methanol maser here, to a limit of 0.3 Jy over most of the velocity range. 337.920 – 0.456 is a new weak OH maser, which does have a methanol maser counterpart (referred to as 337.92 – 0.46 by C + 95).

337.997 + 0.136. The spectra in CHG80 show 1667-MHz peak emission 1.5 times larger than at 1665-MHz, whereas in 1994 it had become much weaker. Detailed comparisons of spectra over nearly 20 yr show large intensity variations of several spectral features at both transitions.

338.925 + 0.557. The strong 1665-MHz emission in the present 1994 observations was even stronger in the spectrum of 1978 shown by CHG80. There is no detectable 1667-MHz emission, but there is 1612-MHz OH maser

emission comparable with the 1665-MHz intensity (Robinson, Caswell & Goss 1974), and shown by S + 97 to be offset by only ~ 1 arcsec from the 1665-MHz position. At 1720 MHz, emission was detected by Robinson et al. (1974), but was very weak; however, a prominent, presumably variable, 1720-MHz maser has been detected recently (MacLeod 1997). 1720- and 1612-MHz masers tend to be mutually exclusive, and it will be important to measure more accurately the position at 1720 MHz. Likewise, a more precise position is needed for the 6035-MHz maser emission in this direction (Caswell & Vaile 1995). Also in this direction is a methanol maser reported by C + 95, and it has been investigated with the ATCA and found to comprise two sites, separated by 30 arcsec. The weaker (5-Jy) methanol maser coincides with the 1665-MHz maser site. Since there appears to be a correlation (Sections 5.4 and 5.6) where 1720-MHz masers generally have accompanying methanol masers but 1612-MHz masers do not, we might expect subsequent position measurements to show the 1720-MHz emission coinciding with 1665-MHz and methanol emission, in which case it might be that the 1612-MHz emission, though very close, corresponds to a distinctly different site.

339.053 – 0.315. This new OH maser is weak, and its nominal displacement of 1.7 arcsec from a methanol counterpart (C96a) may result from the larger-than-usual position error expected for a weak source.

339.282 + 0.136. This is a new OH maser with methanol counterpart (C96a).

339.622 – 0.121. The 1665-MHz OH spectrum in 1994 March remains similar to that in 1978 (shown by CHG80), apart from the disappearance of a 5-Jy feature at velocity -40 km s^{-1} . OH masers at 6035 MHz (Caswell & Vaile 1995) and 1720 MHz (MacLeod 1997) also lie in this direction, but have poor positional accuracy. Methanol in this direction does coincide with the 1665-MHz maser to better than 1 arcsec, and thus it will be interesting to discover whether the 1720-MHz maser precisely coincides with the methanol site, and shows the same close relationship for these transitions that is found in several other sources (Sections 5.4 and 5.6). Note that the nearby strong 1612-MHz maser noted by CH75, is distinctly offset from the methanol and OH 1665-MHz site, by nearly 20 arcsec (S + 97).

339.682 – 1.207. As reported by CVF95, the OH maser has features distributed over 2 arcsec, and two positions are cited in Table 1. Since their separation corresponds to only 23 mpc (for a distance of 2.4 kpc) it seems plausible that the two OH components are part of a single maser site. New ATCA methanol data reveal that there is weak methanol emission (5.8 Jy peak) at a velocity of -34 km s^{-1} which lies (spatially) between the OH features, and thus is most likely from the OH site. The new methanol data also confirm the CVF95 result, that the bulk of the methanol in this general region, including a strong 70-Jy feature, is from a second site, not at the OH position, but offset at least 3 arcsec south of the 'boundary' of the OH. Continuum data at 6.7 GHz (Caswell, unpublished) suggest that a uCH II region of 9 mJy is at the OH site, whereas the site showing only (strong) methanol has no detectable continuum emission.

339.884 – 1.259. This site is 12 arcmin from the previous one, and is thus in the same general SFR, but not closely associated with it. As reported by CVF95, OH maser spots

are spread over more than 1 arcsec, and positions for two features are given; the very strong methanol emission is at a position straddled by the extreme OH positions. All the maser spots are projected on to a uCH II region of 14 mJy (Ellingsen et al. 1996a). The H₂O maser position (FC89) also lies within 0.4 arcsec of the newly measured OH position. (The OH position from FC89 should be disregarded in these comparisons since it has an error of several arcsec, as shown by CVF95.)

340.785 – 0.096. Methanol and 6035-MHz OH masers at this remarkable site are discussed in detail by C97. The present data confirm that emission from the 1665-MHz transition coincides with the methanol and 6035-MHz OH. The velocity range at 1665 MHz is wide, from -108 to -88 km s^{-1} , matching one set of methanol features. In contrast, no 1665-MHz emission lies in the range from -108 to -112 km s^{-1} where an east–west line of methanol features occurs without a 6035-MHz counterpart; this methanol perhaps corresponds to a distinct, different, site despite its spatial proximity, with a projected separation of less than 1 arcsec. According to CH83a, 1720-MHz emission of 1 Jy (LHCP) is present in the region, but a better position measurement is needed to ascertain whether it is closely related.

343.127 – 0.063. The current spectrum is similar to that shown by CH83a, but a weak 1665-MHz feature now present at velocity -40 km s^{-1} was not previously visible. Strong 1612-MHz emission, with a peak of 28 Jy, has been reported here (Caswell et al. 1981; CH83a). It is absent from the S + 97 survey, presumably because it is a narrow single feature and failed to meet the criterion of being detected in at least three spectral channels. It is desirable to determine its position; if it does coincide with the 1665-MHz emission, it would be another example of an OH maser site with a 1612-MHz maser and no methanol maser ($< 0.3 \text{ Jy}$ in C + 95).

344.227 – 0.569. This maser is highly variable, with emission at 1665 MHz 4 times stronger in 1993 February than in 1995 February, and even stronger in the earlier spectrum shown by CH83a. When measured at both 1665 and 1667 MHz, the latter has been several times stronger – most recently strongest near velocity -32 km s^{-1} , but a feature near -23.5 km s^{-1} has also been observed on two occasions. A strong methanol maser coincides (C + 95; CVF95) with the OH maser.

**344.929 + 0.014.* The 1667-MHz maser reported here (with no detectable 1665-MHz counterpart) arises from an OH/IR star that is more than 10 times stronger at 1612 MHz (Caswell et al. 1981), and the 1612-MHz position (S + 97) agrees well with the present 1667-MHz measurement.

345.003 – 0.224. Spectra at 1665 and 1667 MHz are shown by CH83a. The present data show that the position of these coincides with 6035-MHz OH emission, methanol emission and a uCH II region, as discussed by C97. Strong 1720-MHz emission (43 Jy LHCP listed by CH83a) is present, with position (Gaume & Mutel 1987) also coinciding with the other masers. Note that the strongest methanol emission in the vicinity comes from a different maser site, offset by 3 arcsec (C97).

345.437 – 0.074. Spectra of this new maser (Fig. 1) reveal 1667- and 1665-MHz emission similar in appearance and intensity, covering a wide velocity range. These facts suggest

that the object might be a late-type star. However, it has no *IRAS* counterpart and has not been reported as a 1612-MHz OH maser (S + 97), and provisionally we still group it with masers in SFRs. No methanol, to a limit of 0.5 Jy, is present here (unpublished ATCA observations).

345.494 + 1.469 and 345.498 + 1.467. These two masers are separated by 18 arcsec, and their spectra are shown in Fig. 1. They appear as a blended single source in the discovery spectrum of tC96, which was prompted by a search at what now seems to be an unrelated *IRAS* object 6 arcmin away. In 1990, tC96's spectrum shows 345.494 + 1.469 with a peak at -21 km s^{-1} of 5 Jy (corrected by a factor of 2 for pointing offset) which had fallen to 0.5 Jy by 1996 October, as seen in Fig. 1; however, other features remain near 4 Jy. There is no associated methanol ($< 0.15 \text{ Jy}$) at this position, but a 10-mJy continuum ucH II region appears present (unpublished ATCA data). The second site is of comparable 1665-MHz intensity to the first, but covers a smaller velocity range. It has no associated continuum ($< 10 \text{ mJy}$), and coincides with a newly discovered methanol maser (unpublished ATCA data).

345.698 - 0.090. This OH maser site has been known for 25 yr. Currently the 1665- and 1667-MHz intensities are comparable. Spectra from Robinson et al. (1974) and CH83a are generally similar, apart from a strong 1665-MHz feature at velocity -8 km s^{-1} which faded from 20 to 8 Jy and is now less than 1 Jy. Robinson et al. show strong, circularly polarized, 1612-MHz emission from this direction, and its position, measured to an accuracy of several arcsec by S + 97, satisfactorily agrees with the main-line position reported here. 6035-MHz emission is also present at this site (C97), but there is no detected methanol maser (C + 95).

347.628 + 0.148. The present position agrees well with the 6035-MHz OH and methanol (C97). 1612-MHz OH emission was detected in the single-dish observations of Robinson et al. (1974), but its position is still not well determined since it is absent from the S + 97 survey, presumably because its velocity width is small and because it fails to register in at least three spectral channels. Thus 1612-MHz emission may not precisely coincide with the 1665-MHz site investigated here. If it does coincide, it would be an unusual example of 1612-MHz emission also coinciding with a 6668-MHz methanol maser (see Sections 5.4 and 5.6).

347.870 + 0.014. There are three methanol masers nearby (C + 95), but new ATCA methanol observations show that none precisely matches the OH maser site.

348.550 - 0.979. At this 1665- and 1667-MHz site there are matching masers at 6035-MHz OH and at 6668-MHz methanol (C97). A 1720-MHz counterpart is also present (Gaume & Mutel 1987).

348.579 - 0.920. This new OH maser shows a single feature at velocity -27 km s^{-1} , and has a weak methanol counterpart (ATCA unpublished data) at the same position but at a velocity of -15 km s^{-1} .

348.698 - 1.027, 348.703 - 1.403 and 348.727 - 1.037. The three maser sites are quite distinctly separated in the present observations, though confined within a few arcmin in the same cluster, and blended together in the single-dish observations of CH83a. Methanol masers in the general vicinity were reported by C + 95, and have now been studied with the ATCA (unpublished data). 348.698 - 1.027 has no

methanol, with an upper limit of 0.5 Jy. 348.703 - 1.043 has a 60-Jy methanol counterpart, and is the OH site which was positioned by FC89 for a feature at velocity -11.6 km s^{-1} (the strongest RHCP 1665-MHz feature at the 1983 epoch of their observations, whereas a feature at velocity -16.9 km s^{-1} is now strongest). The 6035-MHz maser reported by Caswell & Vaile (1995) has a poorly defined position, but is most likely from this site. 348.727 - 1.037 is a new OH maser, currently the strongest of the three, and a 90-Jy methanol maser lies at this position.

349.092 + 0.106. The OH emission covers the velocity range from -79 to -91 km s^{-1} . There is nearby methanol maser emission shown by C + 95, and new ATCA data reveal that the weak features more negative than -78 km s^{-1} coincide with the OH, and the other, stronger, features correspond to a second site offset by 2 arcsec and with no OH emission.

350.011 - 1.342. Preliminary observations at Parkes detected a 1-Jy methanol 6668-MHz maser in this direction, but no position measurement has yet been made.

350.113 + 0.095. Methanol emission (C + 95) from the approximate direction of 350.113 + 0.095 is found from new ATCA data to be spread over three sites (two were suggested by C + 95), but none coincides precisely with the OH site.

350.329 + 0.100. This new OH maser has no associated methanol maser ($< 0.5 \text{ Jy}$); the nearby methanol emission reported by S + 93 is found from new ATCA data to be offset from the OH by more than 60 arcsec.

350.686 - 0.491. This is a new OH maser which coincides with a 32-Jy methanol maser reported by vGM95 and with a position now measured with the ATCA.

351.160 + 0.697. Both the current spectra and those of CH83a show that the OH emission at 1667 MHz is twice as strong as that at 1665 MHz. At 1667 MHz there is now a new 3-Jy feature at velocity 0 km s^{-1} , which extends the known velocity range of the emission. Methanol at this site is reported by C + 95.

351.417 + 0.645. This 1665- and 1667-MHz OH maser site corresponds to the well-known ucH II region 'f' in NGC 6334A. An extensive study of 6035-MHz OH and 6668-MHz methanol transitions and continuum has now been made (C97), and 1720-MHz OH maser emission is also present at this site (Gaume & Mutel 1987).

351.775 - 0.536. Not only is this the strongest of the known 1665-MHz masers (CH83a), but it also has a large spread in velocity and is spatially extended over several arcsec. It has associated maser emission at 6035-MHz OH and methanol, which are discussed by C97. Surprisingly, the 1612-MHz OH emission in this direction which was thought by CH83a to be quasi-thermal is now found to be a maser with a precise position (Sevenster et al. 1997a) apparently within the boundary of 1665-MHz and methanol emission (see Section 5.6). The 1720-MHz emission recently reported by MacLeod (1997) requires a more precise position to ascertain whether it, too, is from the same site. Detailed studies of the pronounced variability of the OH and methanol masers have been reported by MacLeod & Gaylard (1996) and Caswell, Vaile & Ellingsen (1995b).

352.630 - 1.067. This new OH maser is several times stronger at 1667 MHz than at 1665 MHz. It coincides with a

strong methanol maser (S + 93; positioned in new ATCA observations).

353.410 – 0.360. This maser site has been studied extensively at the 6035-MHz OH transition, 6668-MHz methanol and the continuum (C97). Unusually strong emission from the 6031-MHz OH transition has also been discovered (Smits 1994). The 1665-MHz position measured here agrees with the other transitions. At 1667 MHz there is absorption and no detected emission, but there is strong 1720-MHz emission peaking at 21 Jy in LHCP (CH83a) with a position confirmed as coinciding with the other transitions (Gaume & Mutel 1987).

353.464 + 0.562. A spectrum at 1665 MHz is shown by CH83a; no 1667-MHz emission is detectable, and the nearby 1612-MHz OH maser referred to by CH83a is from a different position, as can now be recognized from the survey by Sevenster et al. (1997a) which shows it to be part of an unrelated OH/IR star. Methanol reported by C + 95 does coincide with the 1665-MHz maser site (ATCA unpublished data).

354.615 + 0.472. The present data show a velocity range for 1665-MHz emission extending slightly further than that seen in the 1981 spectrum (from CH83a); it also matches strong methanol emission in velocity and position (C + 95; CVF95). A quite strong (2-Jy) 1612-MHz maser in this direction reported by Caswell et al. (1981) is 100 per cent RHCP, like the 1665- and 1667-MHz transitions, and probably coincides with them; however, the position uncertainty remains quite large, 15 arcsec, since it was not measured by Sevenster et al. (1997a), presumably because it is a single, narrow feature. If it does coincide with the other transitions, its coexistence with methanol will be an unusual counter-example to the general anticorrelation (Sections 5.4 and 5.6).

354.724 + 0.300. This maser site has been studied extensively at the 6035-MHz OH and 6668-MHz methanol transitions (C97). The 1665-MHz emission reported here coincides with the other transitions. The large positive systemic velocity indicates a location at large distance, probably in the central bar of our Galaxy (Caswell & Haynes 1982). A spectrum from the Parkes telescope with circular polarization information shows strong emission from velocity 94 to 96 km s⁻¹ in RHCP, and weaker emission from 90 to 92 km s⁻¹ in LHCP, suggesting a systematic shift of 4 km s⁻¹ between the polarizations that could be indicative of Zeeman splitting in a field of 6.8 mG. Caswell & Vaile (1995) infer a similar field from 6035-MHz OH Zeeman splitting.

**354.884 – 0.538.* The 1667-MHz maser has a weak counterpart at 1665 MHz, and arises from an OH/IR star that is 100 times stronger at 1612 MHz (Caswell et al. 1981) and with a position (Sevenster et al. 1997a) agreeing with the present 1667-MHz measurement.

355.344 + 0.147. This maser site has been studied extensively at the 6035-MHz OH transition, 6668-MHz methanol and the continuum (C97). The 1665-MHz position measured here agrees in position with the other transitions. The 1667-MHz transition is most prominent in absorption (CH83a), but there is also weak emission 1/30 of the 1665-MHz peak intensity. This OH maser site is the best known example of pronounced large-scale Zeeman splitting at both 1665 and 6035 MHz, as shown by Caswell & Vaile

(1995). It thus allows an assessment of how much the velocity extent of the masers that we attribute principally to kinematic effects might be corrupted by Zeeman splitting. A first glance at the 1665-MHz spectrum shows a velocity range from 14.5 to 21 km s⁻¹, which would shrink to the range 15.5 to 20 km s⁻¹ if corrected for Zeeman splitting. However, closer inspection shows a weak LHCP feature that extends to velocity 13.5 km s⁻¹, and the corrected range would then be 12.5 to 20 km s⁻¹; thus the size of the range would be unaffected by the correction.

**356.646 – 0.321.* This unusual source was classified as most likely an OH/IR star by CH83a, probably identified with IRC – 30308 (=IRAS 17354 – 3155). New spectra shown in Fig. 1 confirm that 1665- and 1667-MHz emission are of comparable intensity and reveal a velocity range that is larger than could be seen in previous spectra. 1612-MHz emission was shown by Caswell et al. (1981) and by CH83a, but no detection was reported by Sevenster et al. (1997a); it may have been missed because of variability, perhaps exacerbated by confusion with another nearby OH/IR star. Alternatively, the 1612-MHz emission may be extended, quasi-thermal, and not closely related to the 1665-MHz maser site.

357.968 – 0.163. This is a new OH maser site, which coincides with a methanol maser reported by vGM95.

**358.236 + 0.115.* This is an unusual OH/IR star, as discussed by CH83a. The same wide velocity range of emission is seen at 1665, 1667 and 1612 MHz, but the intensity is slightly lower at 1612 MHz than at the main OH lines. Sevenster et al. (1997a) confirm that the 1612-MHz position coincides with the main-line position measured here.

358.387 – 0.482 and weaker companion (strictly, at 358.386 – 0.484). The separation of these features is 4 arcsec, normally a large enough separation to indicate two separate maser sites. However, a weak methanol maser lies between the OH positions and coincides with a uCH II region of 110 mJy. Most likely, all the maser features arise from a single site, which has an unusually large angular extent because it is close to us; accordingly, we have listed both positions under the same source name. Note that, although there is a methanol counterpart, it is not the strong one reported in the vicinity by S + 93, which unpublished ATCA measurements show to be offset by 50 arcsec.

0.496 + 0.188. At this OH maser site there is also a methanol maser (S + 93). The accurate methanol position was determined with the ATCA by Caswell (1996b, hereafter C96b), who had discovered a weak 1665-MHz counterpart with the Parkes telescope. The position of the 1665-MHz maser listed here is from a new ATCA measurement, more sensitive than the survey observations of C96b, which were unable to detect it.

0.546 – 0.852. The velocity widths of the 1665- and 1667-MHz spectra are large. The maser site is believed to be within several kpc of us, and its spatial extent is also large, extending over several arcsec. The methanol maser position lies within 2 arcsec of the OH, a continuum peak lies 2.5 arcsec south, and H₂O lies 2 arcsec north. This scatter in these positions may be another indication of an unusually extended site, rather than a cluster of individual sites.

0.658 – 0.042, 0.666 – 0.035 and Sgr B2 generally. OH mapping of the Sgr B2 complex by Gaume & Mutel (1987) shows several discrete maser sites. Our OH observations

have lower spatial resolution and no polarization information, and do not reliably distinguish all the sites listed by Gaume & Mutel. Furthermore, in this very active SFR it is not yet clear whether some of the sites are abnormally large, or represent blends of several nearby sites, each with its own excitation. We therefore list only those two that are strong and clearly separated in the present observations. The first, $0.658 - 0.042$, has no methanol maser associated (< 0.5 Jy according to Houghton & Whiteoak 1995 and C96b). The second, likewise, has no methanol (< 0.5 Jy), but does have an associated 6035-MHz OH maser (C97).

$5.885 - 0.392$. This is an unusual maser site in several respects, with OH showing a large velocity spread, and associated with a strong H II region of more than 6 Jy. Positions of the OH and H₂O masers have been given by FC89 and discussed by Forster (1993). Zijlstra et al. (1990) also show detailed OH maps, with a spread over 4 arcsec, superposed on the H II region map, and argue that there is a blueshifted outflow of OH. Our new data (which cover both frequencies simultaneously, and with a frequency resolution higher than that of Zijlstra et al.) suggest that a small adjustment of the 1665-MHz positions of Zijlstra et al. (south by 0.8 arcsec) may be needed, and would then better match the 1667-MHz data. Some 1612-MHz OH maser emission is present at this site, but no 6668-MHz methanol masers (C + 95), in keeping with the tendency for these two varieties of maser to be mutually exclusive (Sections 5.4 and 5.6).

$6.048 - 1.447$. The OH maser was first reported by CBJ88 and has now been more precisely positioned. A non-detection of methanol was reported here (C + 95) and corresponds to a search at the new, correct, OH position despite being listed as $6.05 - 1.34$ (the name corresponding to an inaccurate preliminary OH position).

$6.795 - 0.257$. The OH maser was first reported by GMv94 at the site of a 79-Jy methanol maser discovered by vGM95. Our accurate positions of both OH and methanol confirm their coincidence to better than 1 arcsec.

$8.669 - 0.356$ and $8.683 - 0.368$. The first of these masers is listed by FC89 (with a feature at velocity 41.1 km s^{-1} strongest at the 1982 epoch of their observations), who note that there is a strong 890-mJy, associated H II region, and C + 95 note that there is a weak, 5.6-Jy, methanol maser here. The second site, $8.683 - 0.368$, we find to be ~ 60 arcsec from previous one; it was also detected in the unpublished data of FC89 and has a strong, 148-Jy, methanol counterpart (C + 95, with improved position from ATCA unpublished data).

$9.619 + 0.193$, $9.620 + 0.194$ and $9.621 + 0.196$. Three distinct OH maser sites are present within this 15-arcsec region (Forster 1993). $9.619 + 0.193$ is the most southerly, coinciding with a uCH II region of 110 mJy (Garay et al. 1993) and a methanol maser with a peak of 40 Jy. $9.620 + 0.194$ covers a wide velocity range, and is slightly stronger at 1667 MHz than at 1665 MHz. It has no detectable methanol (< 0.5 Jy) and no H II region. $9.621 + 0.196$ is the most northerly site, with OH emission at both 1665 and 1667 MHz, and a weak uCH II region of 19 mJy (Garay et al. 1993). At this site, the 1665-MHz peak intensity has slowly decreased by a factor of 2 over the past 15 yr and, most notably, the strongest known 6668-MHz methanol maser is at this site.

$10.444 - 0.018$, $10.473 + 0.027$ and $10.480 + 0.033$. The

OH here was first detected by Braz & Sivagnanam (1987) and listed as $10.46 + 0.02$, with emission at both the 1665- and 1667-MHz transitions. Positions for several features at both the 1665- and 1667-MHz transitions were reported in CVF95, and have now been reanalysed. Each of the three OH maser sites has a methanol counterpart. $10.444 - 0.018$ is 4 times stronger at 1667 MHz than at 1665 MHz, and has a 25-Jy methanol counterpart. $10.473 + 0.027$ is twice as strong at 1667 as at 1665 MHz, displays a wide velocity range at both transitions, has an associated uCH II region that is extremely compact (< 1 arcsec, with flux density 142 mJy at 15 GHz, reduced to 43 mJy at 4.9 GHz) and a strong and highly variable methanol maser. $10.480 + 0.033$ is detected only as 1665-MHz OH and 6668-MHz methanol maser emission.

$11.034 + 0.062$. A spectrum at 1665 MHz is shown by CH83b, but no ATCA measurement has been made, and the position cited in Table 1 is from FC89. Possibly associated 1720-MHz emission is noted by CH83b but needs a precise position measurement, and a very weak methanol counterpart, 0.7 Jy, is present.

$11.904 - 0.141$. The site has been studied at 6035-MHz OH and 6668-MHz methanol (C97), with positions of these two transitions agreeing well with the 1665-MHz position in Table 1 (taken from FC89, with no new ATCA observation).

$12.03 - 0.04$. Since this 1665-MHz OH maser is weak, no ATCA measurement has been made; Table 1 cites the low-accuracy position from CH83b, whose Parkes observations showed a 1665-MHz peak of 3.1 Jy peak in 1982 February, which subsequently fell to only 0.4 Jy in 1993 July. A weak 1720-MHz OH counterpart was reported by MacLeod (1997), and methanol was reported by C + 95.

$12.216 - 0.119$. A spectrum is shown by CH83b, and the position in Table 1 is from the VLA measurement of FC89 (but note that the reference feature of FC should be 11 Jy at velocity 27.9 km s^{-1} , not 0.8 Jy at 26.8 km s^{-1}). No methanol is present at the OH site, although three methanol sites lie in the same cluster, within about 1 arcmin (C + 95, with positions confirmed in unpublished ATCA observations).

$12.889 + 0.489$. This 1665-MHz OH maser was first reported by CBJ88. A methanol maser coincides with it (C + 95, with improved position from unpublished ATCA data).

$15.034 - 0.677$. This maser site has been studied in detail by C97, showing the close relationship of 6035-MHz OH, 6668-MHz methanol and a uCH II region. Spectra at 1665 and 1667 MHz are shown by Haynes, Caswell & Goss (1976), hereafter HCG76) and the 1665-MHz position in Table 1 is taken from FC89, since no new ATCA observations were available.

5 DISCUSSION

5.1 Classification of the detected OH masers

Most of the OH masers reported here are strongest on the 1665-MHz transition and are believed to be associated with SFRs. However, a few are known, or suspected, to be of a totally different variety, associated with late-type, older, lower mass stars – either OH/IR stars, or protoplanetary nebulae. The 11 objects in this category are $284.177 - 0.790$,

326.518 – 0.633, 326.530 – 0.419, 327.102 – 0.263,
 328.225 + 0.042, 331.594 – 0.135, 337.860 + 0.271,
 344.929 + 0.014, 354.884 – 0.538, 356.646 – 0.321 and
 358.236 + 0.115. They are marked with an asterisk in Table 1, and discussed in the individual notes to sources. In summary, the late-type stars have a velocity spread typically larger than 20 km s^{-1} (interpreted as expansion and out-flow) and, in the case of the OH/IR stars, are usually accompanied by strong 1612-MHz maser emission which is mostly unpolarized. Recognizing these masers is important (so that they are not mistakenly classified as unusual SFR masers), and they are excluded from any statistics discussed in the remainder of Section 5.

5.2 The source list, general

Table 1 is a substantially complete listing of previously known 1665-MHz masers close to the Galactic plane, from longitude 230° through the Galactic Centre to $+13^\circ$ (south of declination -16°). It therefore contains all the SFR masers from the earlier Parkes southern surveys. Some new sources are reported, especially additional sources in clusters where the sources are so close that they could not be distinguished in earlier, low-resolution, single-dish measurements.

Each of the present position measurements in Table 1 refers to a single feature, usually the strongest in a spectrum. The weaker spectral features generally lie within 1 arcsec of this position and are not listed, but if a feature is offset by more than ~ 2 arcsec, it is then listed as a separate table entry. Usually these individually listed masers that lie very close to each other are separate maser sites that are part of a cluster, but in some cases they may simply be components of an unusually extended site – see Section 5.5.4.

Some indications of variability of the OH masers were noticeable from comparisons of the spectra of the present observations with those published earlier; intensity changes greater than a factor of 2 can be recognized, even though the precision is limited by the lower velocity resolution and the absence of polarization information from the new data. Furthermore, remarks on variability in the notes in Section 4 are often supported by additional unpublished Parkes observations over the past decade, and we draw attention in Section 5.5.1 to some sources displaying marked variability.

The velocity range of the strongest 100 sources (with a peak stronger than 2.7 Jy) has a median value of 9 km s^{-1} ; this may be regarded as a ‘typical’ value. It is more meaningful than the median for all sources, since the inclusion of weak sources with sensitivity limitations would systematically underestimate the range. It might be thought that 9 km s^{-1} would be a slight overestimate of the true velocity spread, since some additional dispersion can arise from Zeeman splitting: the 1665-MHz line is split by 3 km s^{-1} in a typical 5-mG magnetic field. Often, however, one of the Zeeman components fails to survive when the splitting is this large (see Caswell & Vaile 1995), and then there may be no net broadening from Zeeman splitting (see notes to 355.344 + 0.147 in Section 4). It is interesting that, for methanol masers, estimates of the median value of the velocity spread (C + 95) range from 9 km s^{-1} (when the weakest 25

per cent are excluded) to 12 km s^{-1} (when only the strongest 25 per cent are considered). Some of the large velocity spreads in C + 95 result from the blending of nearby sources (see C96a and C96b), and so 12 km s^{-1} is a slight overestimate for methanol masers. Thus the velocity spread for methanol masers is very similar to the spread that we find here for 1665-MHz OH masers. OH sources with unusually large velocity spread are discussed in Section 5.5.3.

5.3 The systematic survey region, Galactic longitudes 312° to 356°

Close to the Galactic plane, from galactic longitude 312° and extending nearly to the Galactic Centre, the results constitute a new systematic survey. Apart from the much smaller (synthesized) beam and much improved positional accuracy, the present crucial survey parameters of spectral resolution and sensitivity are not greatly different from those of an earlier survey which used the Parkes 64-m telescope (CH87, and references therein). (For most of the Parkes survey, the rms noise was 80 mJy in each sense of circular polarization during the search made with 4-kHz resolution, but all candidates were then studied with higher resolution and higher sensitivity.) Consequently, the number of new sources that are detected in this region constitute a modest 50 per cent increase (from 92 in the Parkes survey to 139 in the present one). Implications from the new sources for the luminosity function and Galactic distribution are minor and are not explored here, since it is clear that the conclusions reached by CH83a and CH87 will remain largely unaltered. Some preliminary results of the present survey between longitude $330^\circ.8$ and $339^\circ.8$ were used for comparison with a matching methanol survey (C96a); note that the OH intensities cited there are larger than in the present listings, since they correspond to higher frequency resolution – see Section 5.6.

5.4 Other maser transitions of OH

CH83a and CH87 summarized the properties of more than 100 southern OH masers characteristic of SFRs. The 1665-MHz transition is usually strongest, and the 1667-MHz transition is detectable towards 90 per cent of them, with intensity typically (median ratio) weaker by a factor of 3, but showing a large scatter, and occasionally stronger, by as much as a factor of 4. 1612-MHz masers are detectable in about 7 per cent of the sites, and 1720-MHz masers in a similar (but mostly different) fraction of sites. These conclusions were based on single-dish measurements, and the coincidence of the emission at different transitions was subject to position uncertainties exceeding 10 arcsec. Coincidences to higher precision had been measured for only a few sources (Gaume & Mutel 1987). The present data allow us to test the coincidences with high precision for many more sources.

We now confirm that, on the scale of the extent of each maser site (typically 1 arcsec), the 1667-MHz maser spots are indeed intermingled with those at 1665 MHz in virtually all cases.

In some instances, the present precise 1665-MHz positions may also be compared with accurate positions of 1612-

and 1720-MHz masers which have become available from other work.

At least 11 sources in the present sample have possibly associated 1720-MHz masers. In four instances (345.003 – 0.224, 348.550 – 0.979, 351.417 + 0.645 and 353.410 – 0.360) an accurate position from Gaume & Mutel (1987) confirms that the 1720-MHz maser coincides with the 1665-MHz maser. The other seven cases, 306.322 – 0.334, 338.925 + 0.557, 339.622 – 0.121, 340.785 – 0.096, 351.775 – 0.536, 11.034 + 0.062 and 12.03 – 0.04, have weak 1720-MHz emission with positions uncertain to at least 10 arcsec, and require further investigation. We note that all 11 sites have associated methanol 6668-MHz masers (see Section 5.6).

There are nine sources from the present sample with coincident 1612-MHz maser emission, as determined chiefly from the surveys by Sevenster et al. (1997a) and S + 97. It seems significant that at least five of these (331.512 – 0.103, 333.234 – 0.060, 333.608 – 0.215, 345.698 – 0.090, 5.885 – 0.392) do not have detectable 6668-MHz methanol. Thus it appears that conditions favouring 1612-MHz masers may tend to inhibit methanol emission, as discussed further in Section 5.6. However, four of the other 1612-MHz sites do have methanol, notably 323.459 – 0.079 and 338.925 + 0.557 where 1612-MHz emission is strong and methanol emission is weak, 351.775 – 0.536 which has strong methanol but weak 1612-MHz emission, and 330.878 – 0.367 where both methanol and 1612-MHz OH are extremely weak compared with the 1665-MHz OH emission. For three other sites where 1612-MHz emission is probably present (343.127 – 0.063 with no methanol, 347.628 + 0.148 apparently with methanol, and 354.615 + 0.472 apparently with methanol), we still await accurate 1612-MHz position measurements. The 1612-MHz masers that once were thought to be associated with the 1665-MHz masers 339.622 – 0.121 (CH75) and 353.464 + 0.562 (CH83a) are now found to be unrelated to them (see notes for these sources).

Most of the 1665-MHz masers have been searched for maser emission at the 6035-MHz transition of the excited state, with many detections reported (Caswell & Vaile 1995), but most of them are weaker than the corresponding 1665-MHz masers. The 6035-MHz detections from Caswell & Vaile (1995) are listed for 56 sources in Table 1, together with the non-detection upper limits for more than 100 other sources (not previously listed in detail). Some weak 6035-MHz masers have rms position uncertainties of 15 arcsec, and their flux densities in column 13 are enclosed in square brackets to signify that the coincidence with the 1665-MHz maser, though likely, is not yet firmly established. Positions with subarcsecond precision for most of the stronger 6035-MHz masers have recently been obtained (C97). These have now been compared with the present 1665-MHz positions, and show excellent agreement, as remarked for individual sources in Section 4. It is also noteworthy that near several 1665-MHz/6035-MHz pairs, there is an additional 6035-MHz maser (C97) which is clearly separate from the main pair and has no 1665-MHz counterpart detectable as yet. In total, amongst the 74 well-studied 6035-MHz OH masers, there are at least eight such instances where any corresponding 1665-MHz maser emission is weaker or absent. In the longitude range from 230° to

13°, the known 6035-MHz masers with no 1665-MHz counterparts are 311.596 – 0.398, 331.511 – 0.103 and 0.666 – 0.029 (see C97). Thus these three sources, though not listed in Table 1, should be regarded as additional OH masers of the SFR variety.

5.5 Unusual sources in the sample

The small number of masers that are clearly of the late-type-star variety were remarked on in Section 5.1, and here we are concerned only with unusual masers of the SFR type. Individual unusual masers are discussed in the notes for the sources, and members of each unusual category are conveniently summarized here.

5.5.1 Unusually variable sources

Some of the sources appear to have remained remarkably stable over at least 20 yr; however, some have not been observed very often, and so their variability is unknown. In the notes in Section 4, we remark on the high variability of 14 sources. For convenience we list them here: 291.579 – 0.431, 311.94 + 0.14, 316.811 – 0.057, 318.948 – 0.196, 319.836 – 0.196, 320.232 – 0.284, 323.740 – 0.263, 326.77 – 0.26, 327.291 – 0.578, 328.254 – 0.532, 331.278 – 0.188, 337.997 + 0.136, 344.227 – 0.569 and 12.03 – 0.04.

5.5.2 Unusual systemic velocities

Several sources in the longitude quadrant 270° to 360° have positive velocities that have noteworthy implications. These include 311.643 – 0.380, 317.429 – 0.561 and 318.044 – 1.405, for which the implied locations lie outside the solar circle and correspond to unambiguously large distances.

The extremely large positive velocity of 354.724 + 0.300 suggests that it lies close to the centre of the Galaxy, in the Galactic bar.

5.5.3 Unusually wide velocity spreads

The typical spread in velocity for the maser spots at any site (Section 5.2) is 9 km s^{–1} (the median for the stronger sources, i.e., omitting sources where the sensitivity to weak features is poor, and omitting sources that are not of the SFR variety). The following 20 maser sites show a spatial distribution of spots confined to a single small region, but with an unusually wide velocity spread, greater than ~18 km s^{–1}: 300.504 – 0.176; 301.136 – 0.226; 311.643 – 0.380; 314.320 + 0.112; 316.640 – 0.087; 323.740 – 0.263; 327.291 – 0.578; 328.254 – 0.532; 328.237 – 0.547; 332.295 + 2.280; 337.405 – 0.402; 337.916 – 0.477; 340.785 – 0.096; 345.437 – 0.074; 351.775 – 0.536; 354.615 + 0.472; 0.546 – 0.852; 5.885 – 0.392; 9.620 + 0.194; 10.473 + 0.027. The cause of the wide velocity spreads could be any of several interesting phenomena: rapid expansion (or contraction), high-speed ejecta (collimated), or rapid rotation. These alternatives can best be explored further by mapping the maser spots in detail with spatial and velocity resolution higher than that obtained in the present data set.

5.5.4 Unusually extended maser sites and small clusters

As remarked in Sections 3 and 5.2, an individual maser site rarely exceeds 30 mpc in extent. In the absence of accurate distances for many sources, we have generally listed features separated by > 2 arcsec (50 mpc at 5 kpc) as separate entries in Table 1. A criterion using linear separations > 50 mpc would be preferable if accurate distances were known, and borderline separations require careful individual consideration, as is given in Section 4.

For a few of the maser sites the total angular extent is unusually large – probably because the site is quite close to us. Attention is drawn to these sites of larger extent by listing a pair of components under the single site names in Table 1; the largest separation at a single site is 4 arcsec, for the pair of components at 358.387–0.482. Other quite extended OH maser sites (most of them with a pair of features listed) include 339.682–1.207, 330.878–0.367, 333.135–0.431, 335.060–0.427, 339.884–1.259, 351.775–0.536, 0.546–0.852 and 5.885–0.392.

In contrast, the two close sites, 330.953–0.182 and 330.954–0.182 are likely to be separate sites within a small cluster of newly formed stars. The two sites 331.542–0.066 and 331.543–0.066 are, similarly, probably members of a small cluster.

5.6 Comparison with methanol masers at 6668 MHz

The close association of OH 1665-MHz or 1667-MHz masers in SFRs with class II methanol masers (specifically at 6668 MHz) has already been documented by CVF95 for a sample of maser sites, with 28 out of 29 apparent associations confirmed as coincident to within 1 arcsec. In addition to the CVF95 data, positions of many more methanol masers to an accuracy of better than 1 arcsec have now been obtained (C96a; C97 and unpublished data). At somewhat lower accuracy, the Parkes positions (C+95) with rms errors ~ 5 arcsec are available for many methanol sources. Methanol masers from other surveys were reported with positions having rms errors of typically 36 arcsec (E+96) or slightly worse (S+93; vGM95), or with positions not measured (Walsh et al. 1995); where it seemed likely that the methanol might coincide with one of the OH masers studied in this paper, an improved methanol position has been measured and used in the notes in Section 4 (full reports of the methanol measurements will be given elsewhere).

Making use of both published and newly measured unpublished methanol observations, we find that for many of the OH masers measured here, a methanol maser is apparently associated. Where both OH and methanol have been observed with the ATCA, the agreement is usually better than 1 arcsec. Indirectly, this agreement is further evidence for the high accuracy of the positions of both species: although, a priori, it is not known whether the true positions of OH and methanol generally coincide, the fact that they are usually found to do so shows that the errors of each are presumably less than the observed separations, since errors are not likely to reduce the separations systematically. References to methanol counterparts are listed in column 13 of Table 1. In some cases the current methanol position uncertainty of ~ 5 arcsec will require refinement to assess these associations more rigorously.

Note that the Galactic source name of a methanol site (as tabulated in C96a, C96b and C97) may differ from its OH counterpart in the millidegree digit, despite positional agreement to better than 1 arcsec. The precise J2000 coordinates must then be compared to ascertain whether the sites are strictly the same, since there also exist cases where sites with almost identical names are quite distinct, with separations exceeding 3 arcsec.

In summary, 201 of the OH maser sites listed in Table 1 are almost certainly of the SFR variety, and approximately 80 per cent of these have methanol maser counterparts. More precisely, 38 of these have no detectable methanol counterpart, and 119 have coincident methanol counterparts; a further 44 have methanol maser emission within 10 arcsec that still needs further investigation and, most likely, the majority of these will prove to be precise counterparts, but a few will prove to be separate maser sites which merely lie in the same cluster. Outside the range of this survey, the data from C+95 for an additional 63 OH masers show 55 with associated methanol maser emission (slightly overestimated if some do not coincide) and at least eight without – a proportion similar to the more detailed data of the present sample.

Where methanol and OH masers occur at the same site, the ratio of peak methanol intensity to peak 1665- or 1667-MHz OH intensity appears to be a useful parameter to characterize the maser site (C97). However, some caution is needed when evaluating this ratio; the present OH intensities are usually underestimated relative to observations with high velocity resolution (as remarked in Section 3) by, typically, a factor of 0.69. Statistics of the ratio of methanol to OH intensity, R , calculated by C+95 and by C96a are based on high-resolution OH spectra, whereas the present tabulated intensities are derived from lower resolution spectra and would lead to a spuriously high value of R . In particular, high-resolution OH spectra were used by C96a to characterize masers as methanol-favoured or OH-favoured according as R is > 32 or < 8 ; in the absence of a high-resolution OH spectrum, the present peak values of Table 1 should be increased by a factor of 1.45 ($= 1/0.69$) before calculating R in order to make meaningful comparisons. The ratio R after applying these ‘corrections’, is given in column 12 (labelled m/OH) of Table 1. (The ratio is enclosed in square brackets for 44 sites where the methanol position is less precise, and where there thus remains a slight chance that the ratio is inappropriate because the methanol and OH are not at exactly the same site.) The larger of the 1665- or 1667-MHz intensities has been used and, where intensities have varied with time, the larger intensities were again used. The median value of R for the 201 SFR OH-selected masers is ~ 4 . (The values of 3.65 found by C+95 is similar; this is not surprising, since much of the sample was the same but with preliminary data.) The tabulation of R in column 12 of Table 1 allows OH-favoured maser sites, with $R < 8$, to be readily distinguished from the methanol-favoured ones with $R > 32$. This will simplify further investigation of the tendency for OH-favoured maser sites to have more readily detectable uCH₃ counterparts than methanol-favoured sites (C97 and Section 5.7).

As might be expected, the sample of sites that are OH-favoured have higher OH flux densities: 105 OH masers

with $R < 4$ have a median flux density of 4 Jy; the 95 sources with $R > 4$ have a median flux density of 1.6 Jy.

As remarked in Section 5.4, there is some indication that the conditions conducive to 1612-MHz masers are inimical to 6668-MHz methanol masers. It is not clear whether this is related principally to the prevailing radiation field, the temperature, the density, or the chemical composition. However, it is also noteworthy that no 6668-MHz methanol masers have been found in the direction of OH/IR stars whose OH maser emission is predominantly at 1612 MHz, and this is a further indication that the environments required by the two varieties of maser are largely incompatible.

5.7 Association with uCH II regions

H II regions smaller than 100 mpc are commonly referred to as ‘ultracompact’, i.e., uCH II regions. Their association with SFR maser sites has been well studied for a few sources. A subset of sites from Table 1, principally those with accompanying 6035-MHz maser emission, have been studied with preliminary continuum observations (C97), and the resulting 6-GHz continuum H II detections are shown in Table 1. In addition, data are available for a sporadic selection of sources at various frequencies between 5 and 22 GHz (FC89 at 22 GHz; Wood & Churchwell 1989 at 5 GHz; Garay et al. 1993 at 15 GHz; and C96a, C96b and unpublished data at 6 GHz). These observations are also added to Table 1. Despite its inhomogeneity, the resulting data set provides a preliminary indication of the statistics of uCH II detections. If maser sites are broadly categorized as either methanol-favoured or OH-favoured, then the OH-favoured sites tend to have stronger uCH II counterparts (C97). Systematic studies of many more of the sources in Table 1 will eventually reveal the significance of this. Meanwhile, we review two explanations. Most simply, towards methanol-favoured maser sites, the putative embedded star may not be of sufficiently early spectral type to sustain a detectable H II region. However, there is evidence in some cases for an alternative explanation, whereby, in the earliest phase of a uCH II region, the UV photons are mainly absorbed by dust, thus limiting the ionization and reducing the uCH II region radio emission (Reid et al. 1995; Wyrowski et al. 1997). The maser properties could then reveal the evolutionary state. Thus in the early stages, the methanol masers may already be prominent before the emergence of the OH maser emission. Both OH and methanol masers then coexist at an intermediate age and, in the later stages of the H II region development, the 6668-MHz methanol masers may fade first, either as a result of enhanced H II region emission, or reduced molecular densities after expansion occurs.

5.8 Pumping schemes for OH in star-forming regions

There has recently been considerable progress in matching the predictions of pumping schemes to observations. Cesaroni & Walmsley (1991) took into account the lowest 28 energy levels of OH, and with a suitable combination of far-infrared radiation field and line-overlap, were able to account for the masers seen in many of the microwave transitions towards W3(OH). There is now general agreement that line-overlap and far-infrared radiation field are

both essential to a viable pumping scheme and, more recently, Pavlakis & Kylafis (1996a,b) performed a new analysis, again taking into account the lowest 28 energy levels. They adopted more accurate collision rates than had previously been available, and argued that accurate values of these rates are vital to even a qualitative understanding of the maser emission. Whereas Cesaroni & Walmsley made comparisons with microwave observations occurring within the full 28 energy levels considered, Pavlakis & Kylafis caution that meaningful comparisons are restricted to transitions at 1612, 1665, 1667, 1720, 4660, 4751 and 4766 MHz. Unfortunately excluded from this set is the strong maser at 6035 MHz (in the $^2\Pi_{3/2}$, $J=5/2$ state), and it is unlikely to be satisfactorily understood until collision rates are available for higher energy levels, since there is a direct connection from the $^2\Pi_{3/2}$, $J=5/2$ state to the $^2\Pi_{1/2}$, $J=7/2$ state (which lies above the energy levels considered). The availability of observations at 1665 and 1667 MHz (this paper) matching those at 6035 MHz (Caswell & Vaile 1995; C97) should be a major spur to improving the pumping scheme. The rarely detected 6031-MHz line of excited OH is sometimes quite strong (Smits 1994; Baudry et al. 1997), and this also requires extension of current pumping schemes. Pavlakis & Kylafis remark that ‘the observations of OH masers are way ahead of the theoretical interpretation...’, but their new work provides optimism that the gap may soon narrow.

6 CONCLUSION

We have surveyed with high positional accuracy a large number of OH maser sites, chiefly in SFRs, and have shown that small clusters of maser sites are present in a number of fields. There are also some interesting examples of sources that possess a wide velocity spread and yet are confined spatially to a single compact site.

Precise positional comparisons between different OH transitions, and with methanol maser positions, reveal close coincidence in most cases. Selecting these coincident cases for closer scrutiny will allow future exploration of the most common morphology of the 6668-MHz methanol and the 1665-MHz OH maser spots, and will ascertain whether they are usually co-spatial.

Further comparisons of the present precise positions with other maser species such as water, and with uCH II counterparts and IR sources, will also now be possible.

Tantalizing results from preliminary analyses will soon benefit from the new, more complete, large sample of OH masers and extend ways in which the evolutionary development of maser sites may be explored. In particular, it will be possible to further investigate the finding (C97) that OH-favoured maser sites have readily detectable uCH II regions, whereas methanol-favoured sites have less prominent uCH II regions, most likely corresponding to an earlier evolutionary stage but possibly an indication of a less massive embedded star. Many sites, none the less, co-host methanol masers, OH masers and uCH II regions.

These analyses complement previous maser studies which focused on individual maser sites; the latter sometimes resembled the apocryphal search confined to a single ‘street lamp’ [of W3(OH)] for the key to understanding star-forming regions. With the present large sample of good maser positions, our studies are no longer constrained to a single

'lamp', but can be extended to many more; these will enable us to discern the most common varieties and use the masers more effectively in understanding regions of massive star formation.

ACKNOWLEDGMENTS

I thank the engineering and computing staff of the ATNF, whose expertise and assistance made this work possible.

REFERENCES

- Allen D. A., Hyland A. R., Caswell J. L., 1980, *MNRAS*, 192, 505 (AHC80)
- Baudry A., Desmurs J. F., Wilson T. L., Cohen R. J., 1997, *A&A*, 325, 255
- Braz M. A., Sivagnanam P., 1987, *A&A*, 181, 19
- Braz M. A., Scalise E., Gregorio Hetem J. L., Monteiro do Vale J. L., Gaylard M., 1989, *A&AS*, 77, 465 (B + 89)
- Caswell J. L., 1996a, *MNRAS*, 279, 79 (C96a)
- Caswell J. L., 1996b, *MNRAS*, 283, 606 (C96b)
- Caswell J. L., 1997, *MNRAS*, 289, 203 (C97)
- Caswell J. L., Haynes R. F., 1975, *MNRAS*, 173, 649 (CH75)
- Caswell J. L., Haynes R. F., 1982, *ApJ*, 254, L31
- Caswell J. L., Haynes R. F., Goss W. M., 1980, *Aust. J. Phys.*, 33, 639 (CHG80)
- Caswell J. L., Haynes R. F., Goss W. M., Mebold U., 1981, *Aust. J. Phys.*, 34, 333
- Caswell J. L., Haynes R. F., 1983a, *Aust. J. Phys.*, 36, 361 (CH83a)
- Caswell J. L., Haynes R. F., 1983b, *Aust. J. Phys.*, 36, 417 (CH83b)
- Caswell J. L., Haynes R. F., 1987, *Aust. J. Phys.*, 40, 215 (CH87)
- Caswell J. L., Vaile R. A., 1995, *MNRAS*, 273, 328
- Caswell J. L., Vaile R. A., Forster J. R., 1995a, *MNRAS*, 277, 210 (CVF95)
- Caswell J. L., Vaile R. A., Ellingsen S. P., 1995b, *Publ. Astron. Soc. Aust.*, 12, 37
- Caswell J. L., Vaile R. A., Ellingsen S. P., Whiteoak J. B., Norris R. P., 1995c, *MNRAS*, 272, 96 (C + 95)
- Cesaroni R., Walmsley C. M., 1991, *A&A*, 241, 537
- Cohen R. J., Baart E. E., Jonas J. L., 1988, *MNRAS*, 231, 205 (CBJ88)
- Ellingsen S. P., Norris R. P., McCulloch P. M., 1996a, *MNRAS*, 279, 101
- Ellingsen S. P., von Bibra M. L., McCulloch P. M., Norris R. P., Deshpande A. A., Phillips C. J., 1996b, *MNRAS*, 280, 378 (E + 96)
- Forster J. R., 1993, in Clegg A. W., Nedoluha G. E., eds, *Astrophysical Masers*. Springer, Heidelberg, p. 108
- Forster J. R., Caswell J. L., 1989, *A&A*, 213, 339 (FC89)
- Garay G., Rodriguez L. F., Moran J. M., Churchwell E., 1993, *ApJ*, 418, 368
- Gaume R. A., Mutel R. L., 1987, *ApJS*, 65, 193
- Gaylard M. J., Whitelock P. A., 1988, *MNRAS*, 235, 123
- Gaylard M. J., MacLeod G. C., van der Walt D. J., 1994, *MNRAS*, 269, 257 (GMv94)
- Haynes R. F., Caswell J. L., Goss W. M., 1976, *Proc. Astron. Soc. Aust.*, 3, 57 (HCG76)
- Houghton S., Whiteoak J. B., 1995, *MNRAS*, 263, 1033
- MacLeod G. C., 1991, *MNRAS*, 252, 36p (M91)
- MacLeod G. C., 1997, *MNRAS*, 285, 635
- MacLeod G. C., Gaylard M. J., 1996, *MNRAS*, 280, 868
- Pavlakis K. G., Kylafis N. D., 1996a, *ApJ*, 467, 292
- Pavlakis K. G., Kylafis N. D., 1996b, *ApJ*, 467, 300
- Reid M. J., Argon A. L., Masson C. R., Menten K. M., Moran J. M., 1995, *ApJ*, 443, 238
- Robinson B. J., Caswell J. L., Goss W. M., 1974, *Aust. J. Phys.*, 27, 575
- Schutte A. J., van der Walt D. J., Gaylard M. J., MacLeod G. C., 1993, *MNRAS*, 261, 783 (S + 93)
- Sevenster M. N., Chapman J. M., Habing H. J., Killeen N. E. B., Lindqvist M., 1997a, *A&AS*, 122, 79
- Sevenster M. N., Chapman J. M., Habing H. J., Killeen N. E. B., Lindqvist M., 1997b, *A&AS*, 124, 509 (S + 97)
- Smits D. P., 1994, *MNRAS*, 269, L11
- te Lintel Hekkert P., Chapman J. M., 1996, *A&AS*, 119, 459 (tC96)
- van der Walt D. J., Gaylard M. J., MacLeod G. C., 1995, *A&AS*, 110, 81 (vGM95)
- Walsh A. J., Hyland A. R., Robinson G., Bourke T. L., James S. D., 1995, *Publ. Astron. Soc. Aust.*, 12, 186
- Wood D. O. S., Churchwell E., 1989, *ApJS*, 69, 831
- Wyrowski F., Hofner P., Schilke P., Walmsley C. M., Wilner D. J., Wink J. E., 1997, *A&A*, 320, L17
- Zijlstra A. A., Pottasch S. R., Engels D., Roelfsma P. R., te Lintel Hekkert P., Umana G., 1990, *MNRAS*, 246, 217